Titre: Title:	Design and Optimization of Air-Liquid Cooling System for Aerospace Applications
Auteur: Author:	Alireza Masoumipour
Date:	2020
Type:	Mémoire ou thèse / Dissertation or Thesis
Référence: Citation:	Masoumipour, A. (2020). Design and Optimization of Air-Liquid Cooling System for Aerospace Applications [Master's thesis, Polytechnique Montréal]. PolyPublie. https://publications.polymtl.ca/5579/

POLYTECHNIQUE MONTRÉAL

affiliée à l'Université de Montréal

Design and Optimization of Air-Liquid Cooling System for Aerospace Applications

ALIREZA MASOUMIPOUR

Département de génie mécanique

Mémoire présenté en vue de l'obtention du diplôme de *Maîtrise ès sciences appliquées*

Génie mécanique

Décembre 2020

POLYTECHNIQUE MONTRÉAL

affiliée à l'Université de Montréal

Ce mémoire intitulé :

Design and Optimization of Air-Liquid Cooling System for Aerospace Applications

présenté par **Alireza MASOUMIPOUR**

en vue de l'obtention du diplôme de *Maîtrise ès sciences appliquées*

a été dûment accepté par le jury d'examen constitué de :

Marcelo REGGIO, président

Jean-Yves TRÉPANIER, membre et directeur de recherche

Sami AMMAR, membre

DEDICATION

To my lovely sister Atefeh and great parents…

ACKNOWLEDGEMENTS

First and foremost, I would like to express my sincerest gratitude to my lead, and project supervisor Prof. Jean-Yves Trépanier, for accepting me in his research group and giving me the opportunity of working on this project. I would like also to express my appreciation not only for his guidance and sharing his knowledge, but also for his time, kindness, and patience during my studies.

I would like to send my deepest gratitude to my committee members to accept to be a member of the jury, namely, Prof. Marcelo Reggio and Dr. Sami Ammar.

I would like also to thank The Simulation-based Engineering Science (Génie Par la Simulation - GPS) program (a CREATE program from the NSERC) and Pratt & Whitney Canada for their financial support.

I sincerely thank M. Serge Dussault and Dr. Jonathan Brulatout from Pratt & Whitney Canada for their support and advices during the research work.

Finally, I would like to send my deepest and sincerest gratitude to my family for all their support and love, especially my lovely sister Atefeh for encouraging me to reach my goals and to divulge my potentials.

RÉSUMÉ

Pratt & Whitney Canada comme un leader mondial de l'aérospatiale et un des manufacturiers majeurs de moteur d'avions a lancé un projet afin d'introduire une nouvelle technologie et type de moteur unique pour différentes applications aérospatiales. La conception globale d'un moteur exige avoir un échangeur de chaleur afin d'extraire la chaleur du liquide de refroidissement. Comme, le poids est un facteur important pour la conception aérospatiale, donc, concevoir un échangeur de chaleur compact et efficace est toujours un défi pour les concepteurs aéronautiques. Afin de relever ce défi, une méthode d'ε-NTU est implémentée à l'aide de logiciel MATLAB pour résoudre les problèmes reliés aux transmissions de chaleur et de dimensionnement liés à la procédure de conception.

La vérification du code implémenté est effectuée pour un seul point afin de vérifier le fonctionnement du code. En ce qui concerne, l'analyse d'échangeur de chaleur est un problème à multiples facettes qui traite de nombreux paramètres dus à la condition de fonctionnement. La vérification est effectuée pour un refroidisseur intermédiaire (Intercooler) en utilisant la méthode ε-NTU et elle a mis en évidence une différence inférieure à 5%. Ensuite, le code implémenté préliminaire est développé pour résoudre le problème de l'échangeur de chaleur compact.

Premièrement, le modèle développé est appliquée à la surface *CF-7.0-5/8J* prise de littérature. Selon la condition de fonctionnement fournie par Pratt & Whitney Canada, le débit massique d'aire est considéré comme une variable. Donc, les résultats obtenus par la méthode ε-NTU pour la surface sélectionnée seront illustrés le comportement d'un échangeur de chaleur compact en fonction de débit massique d'air.

On observe qu'en augmentant le débit massique d'air, le coefficient de transfert de chaleur global augmente et les dimensions de l'échangeur diminuent. Bien que, pour une faible valeur du débit massique d'air, la perte de pression diminue en raison du frottement du noyau de l'échangeur, dans le cas d'un débit massique élevé, la perte de pression augmente en raison de la vitesse de l'écoulement.

L'augmentation du diamètre intérieur des tuyaux, augmente le taux de transfert de chaleur en très petites quantités grâce à la diminution de résistance thermique conductive à travers la paroi des tuyaux. Donc, l'effet d'augmentation de diamètre intérieur peut être considéré comme négligeable.

L'influence du pas des ailettes et de la distance transversale des tuyaux a été analysée sur quatre surfaces, *CF-7.34* et *CF-8.72*, *CF-8.7-5/8J(a)* et *CF-8.7-5/8J(b)*, deux par deux. L'augmentation du pas des ailettes augmente le coefficient de transfert de chaleur global et diminue la perte de pression, tandis que l'augmentation de la distance transversale des tuyaux diminue le coefficient de transfert de chaleur global et la perte de pression.

ABSTRACT

Pratt & Whitney Canada as a global aerospace leader and one of the major aircraft engine manufacturers has initiated a project to develop new technology and unique engine for different aerospace application. The overall design of an aircraft engine requires having a heat exchanger to extract heat from coolant. As the weight is an important factor in aerospace design, therefore, designing a compact and efficient heat exchanger is always a challenge for aircraft designers. In order to address this challenge, the ε-NTU method is implemented using MATLAB to solve rating and sizing problems related to design procedure.

The single-point verification of the implemented code is performed to verify the functioning of the MATLAB code. As the analysis of the heat exchanger is a multi-faceted problem that deals with numerous parameters due to the operating condition. The verification is performed for an intercooler using ε-NTU method and it demonstrated a difference of less than 5%. Then, the preliminary implemented code is expanded to solve the compact heat exchanger problem.

First, the developed model is applied to the surface *CF-7.0-5/8J* taken from literature. Depending on the operating condition provided by Pratt & Whitney Canada, the air mass flow rate is considered as a variable. Therefore, results obtained by the ε-NTU method for the selected surface will be presented the behavior of compact heat exchanger as the function of air mass flow rate.

It is observed that by increasing air mass flow rate overall heat transfer coefficient increases and exchanger dimensions decrease. Although, for the low values of air mass flow, pressure drop decreases due to the core friction, in the case of high mass flow rate, the pressure drop increases due to the mass velocity.

Increasing the tube inner diameter increases the heat transfer rate in very small amounts dur to the decrease of conductive thermal resistance through the tube wall. Therefore, the effect of increasing tube inner diameter can be considered negligible.

Furthermore, the effect of the fin pitch and transverse pitch were analyzed on four surfaces, *CF-7.34* and *CF-8.72*, *CF-8.7-5/8J (a)* and *CF-8.7-5/8J (b)*, side by side. As a result, increasing fin pitch increase overall heat transfer coefficient and decreases pressure drop, while increasing transverse pitch decrease both overall heat transfer coefficient and pressure drop.

TABLE OF CONTENTS

LIST OF TABLES

LIST OF FIGURES

LIST OF SYMBOLS AND ABBREVIATIONS

Abbreviations

CF	Circular Fin
CHE	Compact Heat Exchanger
FP	Fin Pitch
J	Jameson (Data)
LMTD	Log Mean Temperature Difference
MATLAB	Matrix Laboratory, a commercial software developed by Mathworks
P&WC	Pratt & Whitney Canada
SFC	Specific Fuel Consumption

Symbols

A	Total heat transfer surface area, m^2
A_f	Fin profile area, m^2
A_{fr}	Heat Exchanger frontal area, m^2
A_p	Finn profile area, m^2
C	Heat capacity rate, W/K
c_p	Specific heat at constant pressure, $J/kg \cdot K$
D	Diameter, m
D_f	Fin diameter, m
D_h	Hydraulic diameter, m
f	Friction factor
G	Mass velocity, $kg/s \cdot m^2$
j_H	Colburn-j factor
h	Convection heat transfer coefficient, $W/ m^2 \cdot K$

L_c	Corrected fin length, *m*
L_f	Fin length, *m*
L_{HX}	length of the heat exchanger in the direction of air flow, *m*
$\dot{m}$	Mass flow rate, *kg/s*
N_f	Number of fins
N_L	Number of tubes in the direction of air flow
Nu	Nusselt number
$\boldsymbol{\mathcal{P}}$	Fluid pumping power, *W*
Δp	Pressure drop, N/m^2
Pr	Prandtl number
q	Heat transfer rate, *W*
q_f	Actual heat transfer rate from the fin, *W*
$q_{f,max}$	Ideal heat transfer rate from the fin, *W*
q_{max}	Maximum possible heat transfer rate, *W*
Re	Reynolds number
R_f	Fouling factor, $m^2 \cdot K/W$
R_w	Wall resistance, *K/W*
S_f	Single fin heat transfer surface area, m^2
S_L	Longitudinal pitch of a tube bank, *m*
S_T	Transverse pitch of a tube bank, *m*
ST	Stanton number
T	Temperature, *K*
t_f	Fin thickness, *m*
U	Overall heat transfer coefficient, $W/m^2 \cdot K$

V_{HX}	Total volume of the heat exchanger, m^3

Greek Letters

α	air-side heat transfer surface area per unit volume, m^2/m^3
δ	Fin thickness, m
ε	Effectiveness
η_f	Fin efficiency
η_o	Fin temperature effectiveness
μ	Viscosity, $kg/s \cdot m$
ρ	Density, kg/m^3
σ	Ratio of heat exchanger minimum cross-sectional area to frontal area
υ	Specific volume, m^3/kg
ϕ	Function

Subscripts

c	Cold fluid; cold side
f	fin
h	Hot fluid; hot side
i	Inlet; inner
max	Maximum
min	Minimum
o	Outlet; outer
r	Ratio

LIST OF APPENDICES

CHAPTER 1 INTRODUCTION

1.1 Context

Pratt & Whitney Canada (P&WC) as a global aerospace leader and one of the major aircraft engine manufacturers has initiated a project to develop new engine technology for different aerospace applications. The objective of P&WC is to introduce an efficient new engine leads to extend operating rang, reduce fuel consumption, lower operating cost, and higher and faster missions. This new technology can be used in three different markets. The application can be considered for small-scale operators (helicopters and working-class aircraft), large-scale operators (Auxiliary Power Unit) and individual operators (general aviation).

As a major project at P&WC, the project is divided to several parts to design different components such as compressor, turbine, combustion chamber, fuel system, intercooler, cooling system, etc. Therefore, each component and system are referred to the related department to perform and continue the design procedure.

As mentioned above, the overall design of an aircraft engine requires having a cooling system to extract heat from coolant. Like all components of aircraft engine, cooling system can be designed as efficient as possible to help improving engine thermal efficiency, as well as reducing fuel consumption. Thus, design of cooling system can be defined as a sub-project within the framework of global project. Despite all previous designed and existent cooling systems and technologies, in the framework of cooling system design project, P&WC collaborates with Polytechnique de Montréal to find a solution for cooling system design and perform a study on rating and sizing problem of heat exchanger.

The cooling system design project in overall vision is an industrial project to design and optimize a complete thermal system including heat exchanger and a blower for the aerospace application. Aerospace industries are always seeking continuous improvement in their products in terms of performance, efficiency, weight, etc., and in the meantime reduce cost of production. As, the function of heat exchanger is to perform the exchange of heat between two fluids at two different temperatures [1], therefore, heat exchanger is required for any kind of internal combustion engines, such as Reciprocating, Rotary and Continuous Combustion engines. To reduce the overall weight of engine as well as aircraft, each component will be designed as light as possible, to reach this

goal. The design of heat exchanger follows the same rule. Therefore, the cooling system should be considered as compact as possible. To do so, a Compact Heat Exchanger (CHE) will be designed to overcome the generated engine heat. The cores of typical CHEs are represented in Figure 1.1.

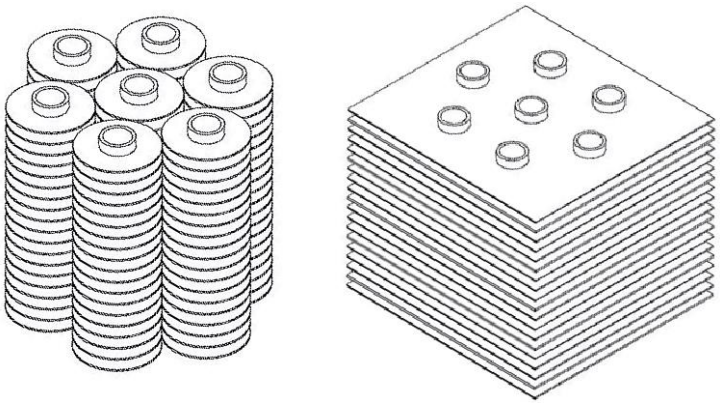

a) Circular tubes, circular fins b) Circular tubes, continuous plate fins

Figure 1.1 Cores of the typical compact heat exchangers [1]

Furthermore, the perspective of the sub-project, including CHE and blower modules, is illustrated in Figure 1.2. This thesis deals with thermal part of the cooling system project and focus on design and study of the characteristics of the CHE.

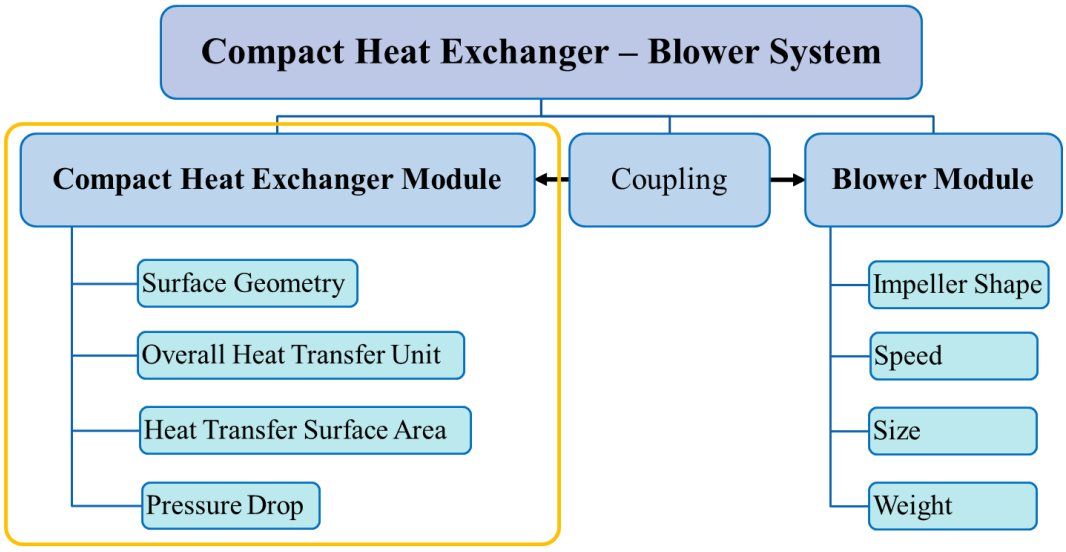

Figure 1.2 Compact Heat Exchanger-Blower coupled system

The heat exchanger enhances the heat transfer rate by increasing the power and fluid flow velocity. Another parameter plays a significant role in design of a heat exchanger is the cooling airflow generated by a blower or a fan. The design of a CHE needs the consideration of heat transfer rate and the power that expand the liquid inside the CHE to overcome fluid friction. Therefore, using CHE enhances the heat transfer rate by increasing the power and fluid flow velocity [1, 2].

One of the most important objectives in aerospace applications, especially for the CHE design, is to reduce global weight to improve engine performance which leads to reduce fuel consumption. To obtain such information, first, a mathematical model of CHE should be developed. Then, based on acquired results, the optimum design of the compact heat exchanger can be chosen with respect to compact heat exchanger inlet and outlet temperature.

Design of efficient CHE needs to determine the flow rate generated by the blower. The design of a high-performance blower requires experience of designer. To do so, for a given design point, Cordier diagram serves a promising tool to determine the main dimensions of the blower. The Cordier diagram by Cordier (1955) is obtained based on the experiment results and analysis of different turbomachines to correlate data to represent the relation between diameter, pressure, and flow rate. Cordier presented a relation between non-dimensional parameters which are specific speed, N_s, and specific diameter, D_s, for different classes of turbomachines. This diagram is useful for blower design procedure. Since the range of rotational speeds for different turbomachines are know from experience, rotor diameter can be calculated from specific diameter based on input data such as air volumetric flow rate and head of machine. Cordier had represented a set of rules and guidelines to design and selection of turbomachines. However, the Cordier diagram does not serve as a tool for blade shape design. The Cordier diagram is illustrated in Figure 1.3 [3-6].

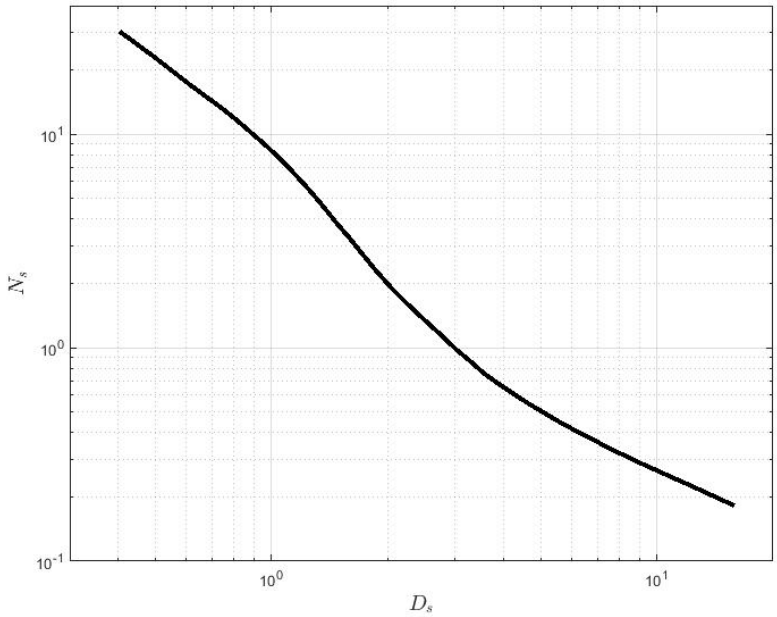

Figure 1.3 Cordier diagram [5]

Design and investigation on blower are not included in this study.

1.2 Problem Definition

The design of the heat exchanger is complex and requires considering of numerous variables and parameters. The optimization of a compact heat exchanger is still controversial due to the complex design processes. Considering the design procedure, which is associated to various parameters, optimization techniques provide a brilliant framework to achieve an augmented outcome. For this purpose, many works have been well established by using an iterative approach with trial-and-error process with respect to specific requirements [7, 8].

Heat exchanger thermal design problems consists the rating and sizing problems which are two of simplest and most important problems. The rating problem refers to the determination of heat transfer characteristics and pressure drop of either existing or already sized heat exchanger. Thus, the outlet temperature, overall heat transfer coefficient and pressure drop are the result of rating problem. On the other hand, sizing problem for exchanger with extended surface refers to the determination of physical size of heat exchanger. Therefore, the design task will be the consideration of surface geometry, flow arrangement, materials, etc., as described in the literature [9, 10].

P&WC is looking for an air-liquid cooling system to optimize installed weight. Moreover, this project forms a part of the company strategy for investigating and developing new technologies for different kinds of powerplants that give the potential for significant improvements in fuel consumption versus current gas turbine aeroengines.

The design problem and the investigation on rating and sizing problems will be performed by using P&WC's input data such as hot fluid properties and inlet and outlet temperatures as well as the quantity of heat to be extract and cold fluid temperature.

1.3 Objectives and Proposed Study

This study consists studying various configurations of circular tube-circular fin compact heat exchangers that aims to perform a mathematical simulation to determine optimum effectiveness versus pressure drop and total volume which are related to the total installed weight.

In order to achieve the principal goals of the project, specific objectives have been set as follows:

- Consider an existing exchanger (surface: *CF-7.0-5/8J*) as the reference CHE for developing a MATLAB code.
- Determine the characteristics of exchanger using implemented code.
- Verify MATLAB code results versus analytical solution presented in literature.
- Update and expand the MATLAB code to simulate and solve rating and sizing problem as well as study of pressure drop.
- Perform a sensitivity study on surface geometry (fin and transverse pitch)

1.4 Thesis Outline

This thesis contains 6 chapters. First chapter present the overview of the project presented by P&WC and the objectives. Second chapter presents the literature review on heat exchangers along with state-of the-art in CHE design and optimization. Chapter 3 will introduce the methodology on current work. Verification the implemented code for heat exchanger with analytical results will be discussed in chapter 4. Results will be discussed in fifth chapter followed with a conclusion and recommendations in chapter 6.

CHAPTER 2 LITERATURE REVIEW

A heat exchanger is a device that process exchange of heat between two or more fluids with different temperatures. Numerous models of heat exchangers have been introduced to be used in any kind of industry, especially in aerospace and defense industries [11, 12].

2.1 Heat Exchangers and Classification

Typical application of heat exchanger can be resume as cooling and heating of fluid stream. The other applications can be performed as recover or reject heat, concentrate, distil, crystallize, pasteurize, or control a process fluid. In heat exchangers, the exchange of heat associates with convective and conductive heat transfer over separating solid wall between two fluids. However, in some heat exchangers, the heat exchange between fluids is in direct contact. Heat exchangers, in which fluids are separated by the heat transfer surface, assign to Direct Transfer Type or Recuperators. In other hand, there is heat exchanger with an energy storage. In this kind of heat exchangers, both hot and cold fluid flow over the core of heat exchanger which is an energy storage and dissipation unit. In this kind of heat exchanger, the core of heat exchanger, which is called Matrix, store the heat brought by the hot fluid. To conclude this process, the hot fluid will be replaced by cold fluid and the matrix will transfer this heat to the cold fluid. This type of heat exchangers called Indirect Transfer Type or Regenerator. The other type of basic heat exchangers is Direct Contact Heat Exchanger in which cold and hot fluid or gas are in direct contact to each other to exchange the heat. The simplest example of this kind of heat exchangers is the cooling tower in which hot fluid is falling and cooled by direct contact with cold air stream upward. In heat exchangers, if there is no phase change during heat transfer process in any of fluids, it can be referred to Sensible Heat Exchanger. In such exchangers, there could be the internal energy sources such as nuclear fuel elements or electric heaters [9, 13].

Heat exchangers can be classified according to the different categories such as:

- Construction
- Transfer process
- Flow arrangement

The above-mentioned classification of heat exchangers can be seen in Figure 2.1.

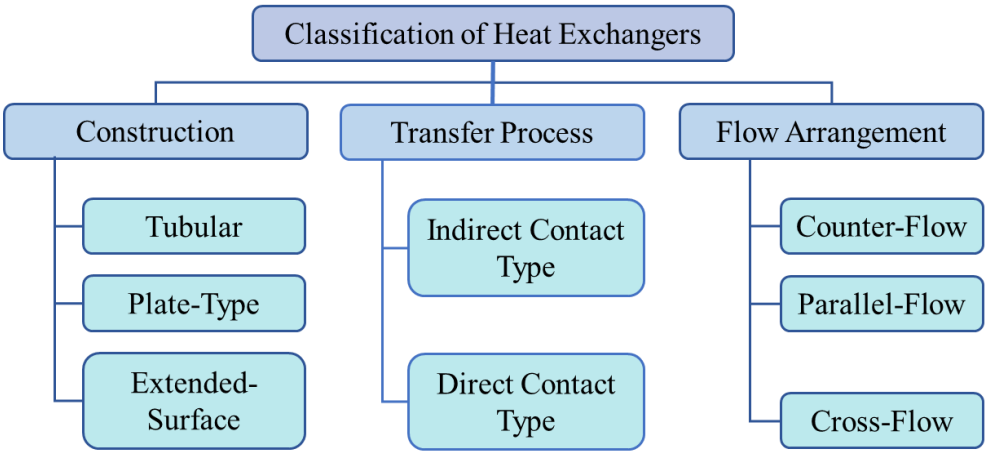

Figure 2.1 Classification of heat exchangers [9]

The introduction to classification illustrated in Figure 2.1 will be briefly presented in following sub-sections.

2.1.1 Classification According to Construction

Heat exchangers can be classified by construction features. Three major classifications based on construction can be named as tubular, plate-type, and extended surface. Although, the other construction such as cooler cartridge, tank heater and scraped surface exchanger are available, their applications are specialized [9]. Therefore, we will focus on three major construction mentioned above.

2.1.1.1 Tubular Heat Exchangers

Tubular heat exchangers are commonly constructed with circular tubes, however, in some applications, other type of tube geometries such as rectangular, elliptical, etc., can be used. The advantage of this kind of heat exchangers is design flexibility due to the core geometry that can be changed by tube diameter. Tubular heat exchangers are primarily used for liquid-to-liquid and liquid-to-phase change applications. Phase change application may consider as evaporating or condensing. The other applications of this kind of heat exchanger construction are for gas-to-gas and gas-to-liquid when either operating pressure and temperature or one of them is very high [9]. Tubular heat exchangers can be classified as follows:

- Shell-and-tube heat exchangers

Shell-and-tube is the common type of heat exchangers that used mostly in chemical and process industry; therefore, more than 90 percent of heat exchangers used in industries are the shell-and-tube. In this type of exchangers, a bundle of tubes mounted inside a cylindrical shell. The heat transfer process occurs between the fluid inside tubes and fluid flow across and along tubes. Shell-and-tube exchangers can be considered as the first choice in industries due to the straightforward and well-established design procedure. Moreover, manufacturing process, variety of materials and availability of codes and design standards are the reason to choose this type of heat exchanger. Theoretically, there is no limit of operating pressure and temperature for shell-and-tube heat exchanger. On the other hand, shell-and-tube exchanger can be classified as non-compact heat exchangers, due to the lower value of heat transfer surface area per unit volume (α). Therefore, shell-and-tube exchangers require support structure, considerable amount of space and expensive installation costs [9, 10, 13-15]. A shell-and-tube exchanger is shown in Figure 2.2.

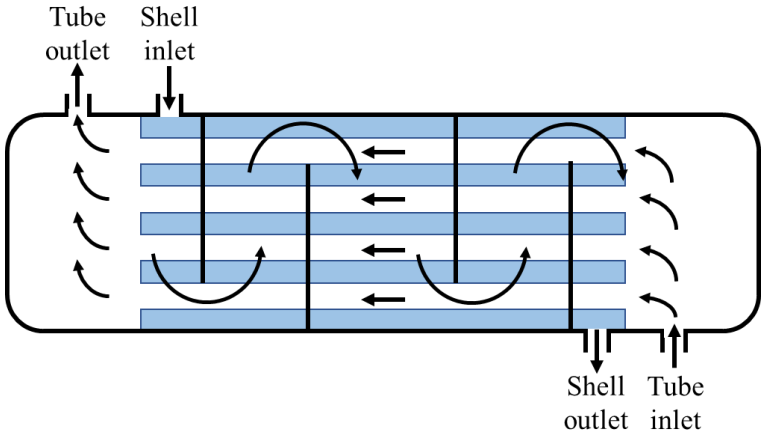

Figure 2.2 Shell-and-tube exchanger with one shell pass and one tube pass [1]

- Double-pipe heat exchangers

Double-pipe heat exchanger consists of two concentric tubes with inner finned or plain pipe and in U-bend design. The flow arrangement in double-pipe heat exchangers is generally countercurrent. In double-pipe exchangers, one fluid flows in the inner tube and the other fluid flows between two pipes in the counterflow direction for the highest performance per heat transfer surface area. In some cases when the constant wall temperature is required for

the exchanger, both fluids may flow in the same direction (parallelflow). Double-pipe heat exchangers are suitable for high pressures and temperatures and thermally long duties. This kind of exchangers are not very compact [9, 10, 16].

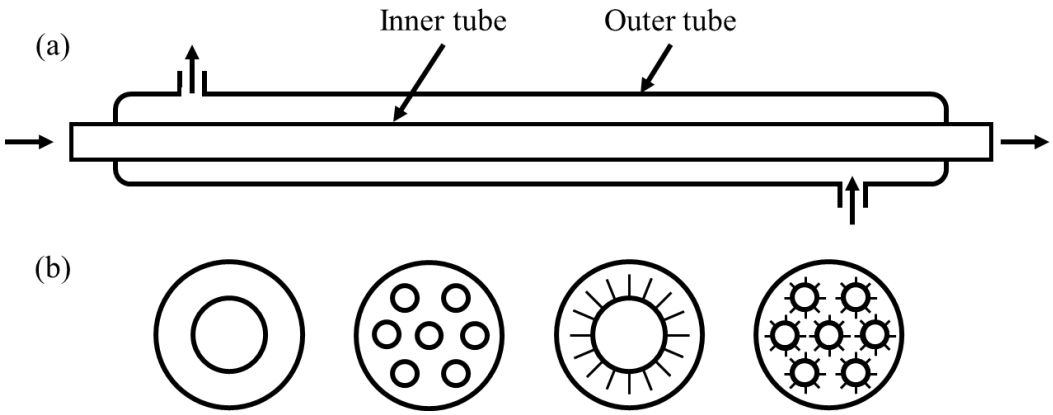

Figure 2.3 Double-pipe heat exchanger. a) Schematic of unit, b) Various internal tube configurations [10]

- Spiral tube heat exchangers

  This kind of exchanger consists of one or more spirally wound pipes inside a shell. The heat transfer rate associated with spiral tube heat exchangers are generally higher than the straight tube [9].

2.1.1.2 Plate-Type Heat Exchangers

Plate-type of heat exchangers are generally constructed with thin plate. There is usually some shape and pattern of corrugation on plates. The plates can be flat or wound inside the heat exchanger. Plate-type heat exchangers are generally cannot adapt with high pressures and temperatures, therefore, less extensively employed than tubular exchangers. Plate-type heat exchangers can be classified in following groups:

- Gasketed (plate and frame) plate heat exchanger

  This model of plate-type heat exchanger can be adapted for medium pressure liquid-to-liquid heat transfer applications. Gasketed plate exchangers are an alternative for tube and shell heat exchangers. In this model, each plate is built with four ports as inlets and outlets. All plates are clamped together to create a flow passage. The thermal control required for

pasteurization and ease of cleaning make this kind of heat exchanger ideal for pharmaceutical industries, general food processing, dairy and beverage industries, alcoholic drink, etc. The main disadvantages of plate and frame exchangers are vulnerability to leakage due to the gaskets and high-pressure loss because of small diameter of passages which makes this kind of exchanger costwise in terms of pumping system. A schematic of gasketed heat exchanger is illustrated in Figure 2.4 [9, 10, 14].

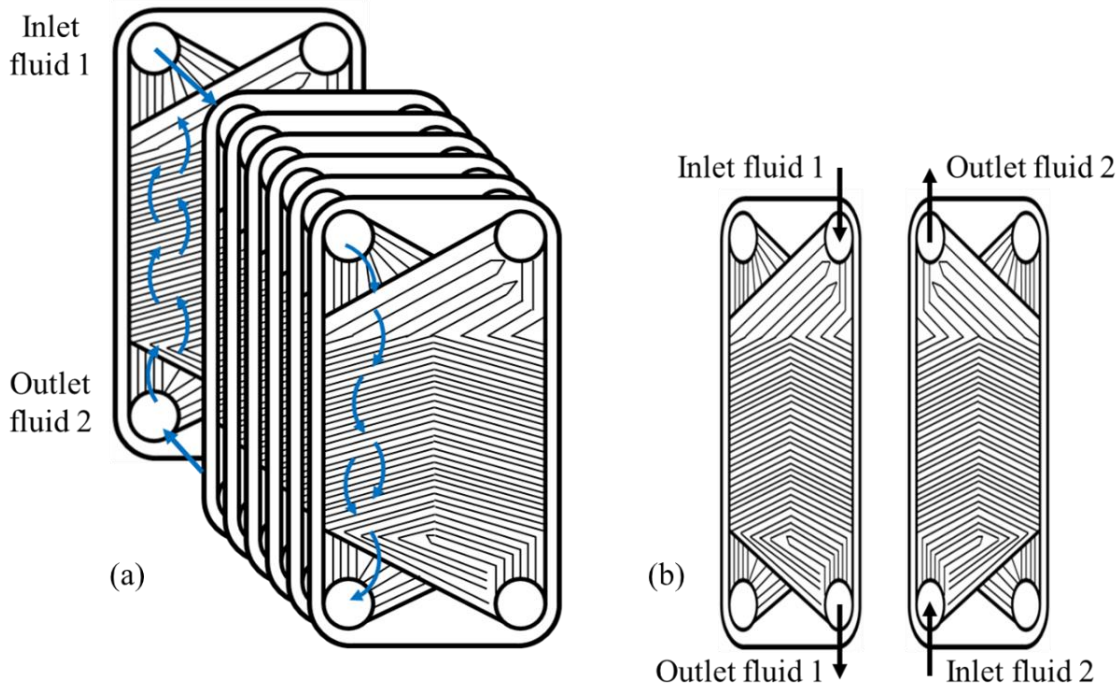

Figure 2.4 a) Gasketed plate and frame heat exchanger. b) Plates illustrated gasketed around the ports [9]

- Spiral plate exchanger

  Spiral plate heat exchangers were introduced during 1930s, where they were developed in Sweden for heat recovery. This type of exchanger can be classified as welded plate heat exchangers. Spiral plate heat exchangers are fabricated with two strips of sheet metal and wrapped helically, and each fluid has its own passage. the spiral heat exchangers generally have large diameters due to the spiral turns. This kind of exchanger can be used for extremely high viscosity fluids and is suitable as reboiler and condenser [9, 10].

2.1.1.3 Extended-Surface Heat Exchangers

In many applications of heat exchangers unlike tubular and plate-type exchangers in which the effectiveness is usually about 60%, the higher effectiveness up to 98% is required. Moreover, in some applications more compact surface, and limited installation space are design constraints. Also, in heat exchanger applications where the overall heat transfer coefficient is low in one or both fluid sides, thus, large heat transfer surface area is the requirement. Therefore, the most prevalent method to raise heat transfer surface area is to add extended surface in one or both fluids sides of exchanger. Although, the overall heat transfer coefficient in extended surface exchangers can be lower or higher than unfanned exchangers, using fins can increase heat transfer surface area by 5 to 12 times. Interrupted fins can provide increase of heat transfer surface area and overall heat transfer coefficient. Internal fins inside tubes, increase the surface area, however, it can marginally reduce the heat transfer coefficient depending fin spacing. Therefore, it can be concluded that, in general, increase of fin density may result in heat transfer coefficient reduction associated with fins. Plate-fin and tube-fin exchangers are two common models of extended surface heat exchangers as illustrated in Figure 2.5 [9, 10].

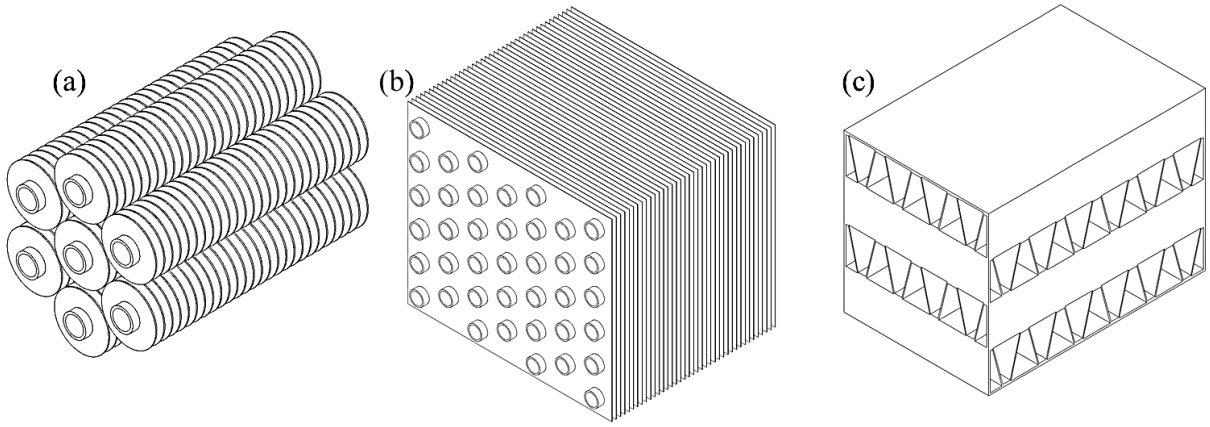

Figure 2.5 Plate-fin and tube-fin heat exchangers. a) Tube-fin (circular tubes, circular fins). b) Tube-fin (circular tube, continuous plate fins). c) Single pass plate-fin [1, 10]

- Plate-fin heat exchanger

  In this type of heat exchangers, extended surfaces or fins are in rectangular or triangular cross-section shape which are placed between parallel plates. Plate-fin exchangers are commonly employed for gas-to-gas heat transfer as they provide high area densities. This

kind of exchanger is designed and used for low-pressure applications. Moreover, the operating temperature is limited to the type of material employed. The other advantages of plate-fin heat exchangers can be named as the low weight per heat transfer surface area and possibility of heat exchange for variety of process streams, lower equipment weight for a given volume and better heat transfer per surface area [9, 10, 15, 17]. Basic components of plate-fin exchangers are illustrated in Figure 2.6.

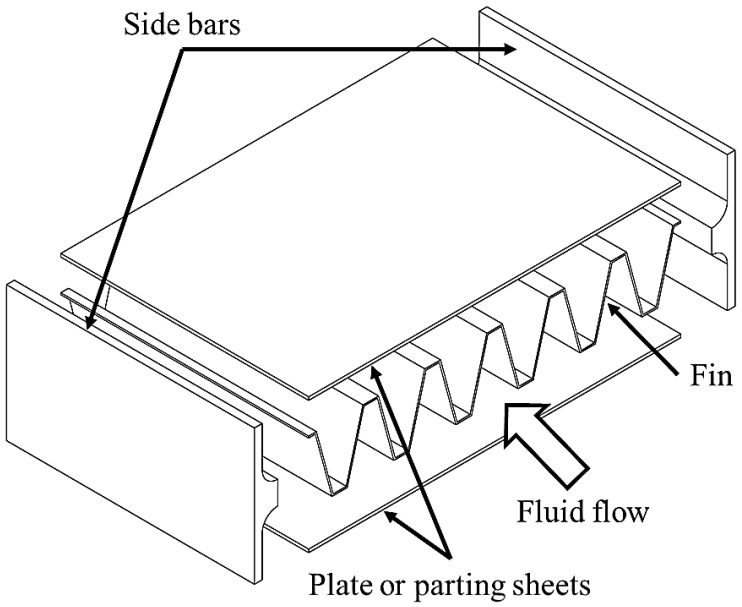

Figure 2.6 Basic components of plate-fin exchangers [9, 15]

- Tube-fin heat exchanger

  This type of heat exchangers is commonly employed in variety of applications. Generally, they are used when the fluid flow pressure or overall heat transfer coefficient (or both) are significantly higher than the other fluid flow. As an example, in gas-to-liquid heat exchangers, the overall heat transfer coefficient in liquid side is very high compared to gas side, therefore, the extended surface (fins) is added to the gas side to increase the heat transfer surface area to enhance heat transfer rate. Generally, tube fins exchangers have less compactness than plate fins exchangers. It can be design for variety of tube fluid operating pressures when the other fluid operates at low pressure [9, 10, 15]. In this category of heat exchangers, fins outside of tube can be classified as follows:

- Individually finned tubes in which normal fins are attached to the individual tubes as Figure 2.7(a) [10].
- Longitudinal fins attached to individual tube as illustrated in Figure 2.7(b). This type of fins is commonly employed for viscose fluids and condensing applications [10].
- Continuous or flat fins normal to the tube bank as represented in Figure 2.5(b) [10].

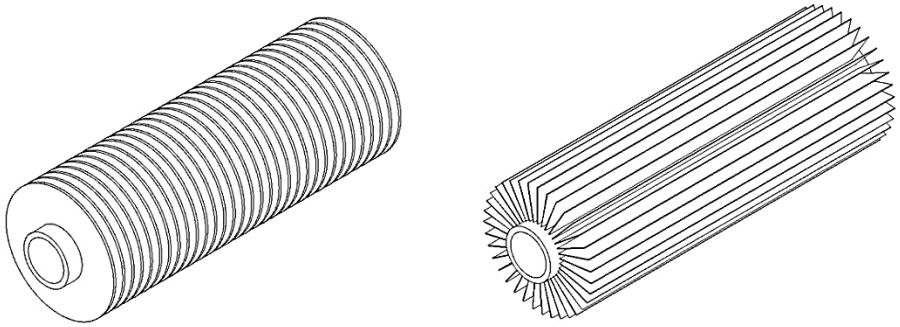

Figure 2.7 Tube-fin exchangers. a) Normal circular fins on individual tube. b) Longitudinal fins on individual tube [10]

2.1.2 Classification According to Transfer Process

Heat exchangers can be classified by the type of transfer process. In this regard, they are classified into indirect- and direct- contact types.

2.1.2.1 Indirect-Contact Type

In indirect-contact type exchangers, fluids flow inside the exchanger are separated with a separating wall. In this exchanger, which is called also surface heat exchanger, there is no direct between fluids streams. Indirect-contact exchangers can be further classified into storage type, fluidized-bed, and direct-transfer exchangers which are also called Recuperator. Direct-transfer exchangers are hot and cold fluid flow are through a separating wall with no moving parts. Tubular, plate-type, and extended surface heat exchangers which are mentioned in previous sections are examples of indirect-contact exchangers [9, 10].

2.1.2.2 Direct-Contact Type

In direct-contact heat exchanger, fluids come into the direct contact, exchange heat and separated later. Therefore, fluids are not separated by separating wall. Heat transfer process in this type of exchangers involves mass transfer. The enthalpy of phase change during heat transfer process perform a considerable part of total energy transfer. Moreover, heat transfer rate may be enhanced with phase change. In comparison to indirect-contact heat exchangers, in direct-contact exchanges the construction of exchanger is economical and high heat transfer rate is achievable [9, 10]. Three common type of direct contact exchangers can be represented as follows:

- Immiscible Fluid exchangers
- Gas-liquid exchangers
- Liquid-vapor exchangers

2.1.3 Classification According to Flow Arrangement

Heat exchangers can be classified by their flow arrangement based on required size, fluid flow paths, effectiveness, pressure drop, heat transfer rate, temperature levels and other design criteria. The type of flow arrangement is the important key in design and balance the drop of temperature by obtaining the coefficient of heat transfer on both exterior and interior sides of tubes [9, 10, 12]. The basic flow arrangement in heat exchangers will be discussed in next sub-sections.

2.1.3.1 Counter-Flow Heat Exchangers

In counter-flow (countercurrent) heat exchangers, two fluids are parallel to each other in opposite direction as illustrated in Figure 2.8. Counter-flow arrangement exchangers are thermodynamically superior to other arrangements and the thermal stress is the minimum compared to other flow arrangement dur to the temperature variation through exchanger. Moreover, this type of exchanger performs as the most efficient flow arrangement, since for given overall thermal conductance, it produces the highest temperature change between fluids. One-dimensional temperature distributions in counter-flow for a single-pass exchanger and single-phase fluids are represented in Figure 2.9 [9, 10].

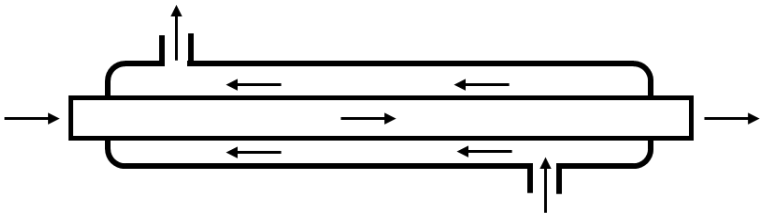

Figure 2.8 Double-pipe exchanger with pure counter-flow [9]

In Figure 2.9, T and C represent temperature in K and heat capacity rate in W/K, respectively. In addition, the subscripts h, c, i and o denote hot, cold, inlet and outlet, respectively.

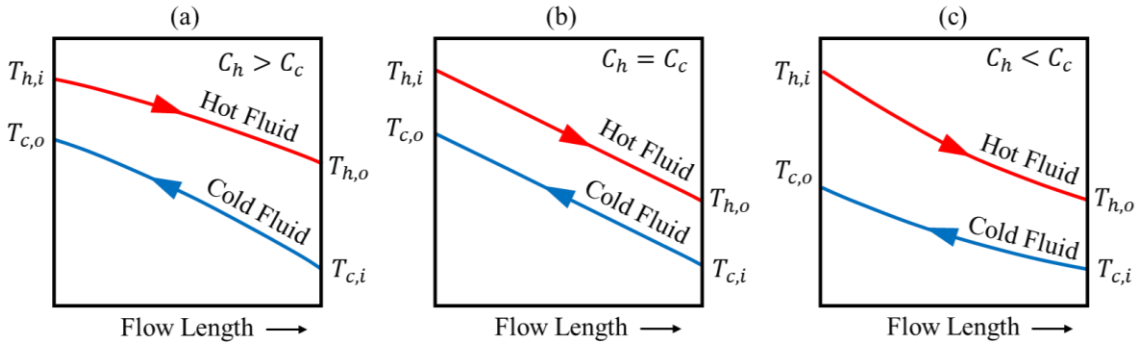

Figure 2.9 Temperature distribution in counter-flow for single-pass exchanger single-phase fluids [9, 10]

2.1.3.2 Parallel-Flow Heat Exchangers

In parallel-flow exchangers which are also referred to cocurrent or cocurrent-parallel stream, both fluids are entered and left the tubes in the same direction as shown in Figure 2.10. this type of heat exchanger produces the lowest effectiveness among the other single-pass exchanger as it represents the minimum temperature variation between two fluids for given overall thermal conductance, fluid inlet temperature and fluid flow rate. Although, the thermal effectiveness of parallel-flow is less than counter-flow, the difference is small. As illustrated in Figure 2.12, the maximum temperature difference exists at exchanger inlet which produce high thermal stress in this area. On the other hand, parallel-flow exchangers provide rapid heating where they are employed for high viscose fluid heating [9, 10].

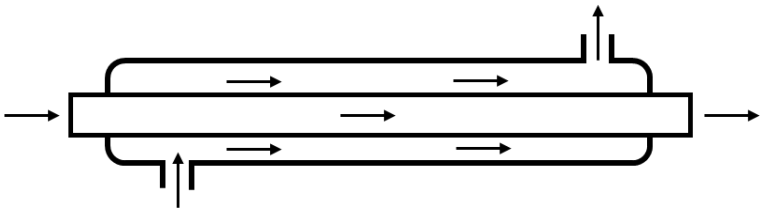

Figure 2.10 Parallel-flow arrangement [12]

One-dimensional temperature distributions in counter-flow for a single-pass exchanger and single-phase fluids are represented in Figure 2.11.

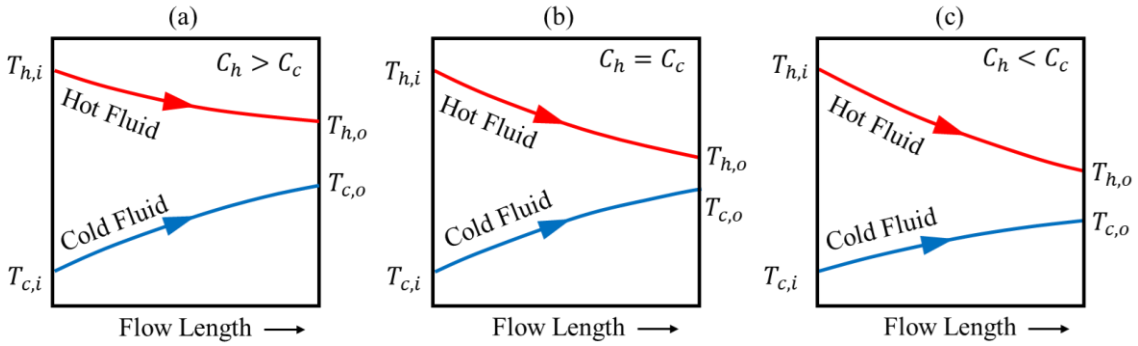

Figure 2.11 Temperature distribution in counter-flow exchanger [9, 10]

2.1.3.3 Cross-Flow Heat Exchangers

The most common type is when two fluids move from each other perpendicularly, the configuration is called cross-flow as illustrated in Figure 2.12. The application of the cross-flow arrangement in heat exchangers extensively are used as air-conditioning, ventilation and heating as a result of the possibility of design, cost, fabrication and maintenance. Moreover, cross-flow arrangement is the common exchanger with extended-surface due to the header design simplicity at entrance and exit. The effectiveness of cross-flow exchangers is between that in counter-flow and parallel-flow arrangement [9, 13, 18].

In cross-flow arrangement, the fluid flow can be considered as unmixed when the fluid flow is through an individual tubes or channels. In this case the fluid flow is in perpendicular direction with fluid flow tubes due to present of the fins that prevent fluid moving along the tubes. On the other hand, mixed fluid flow is considered when the fluid is free to move in transversal direction and no temperature gradient exists in transverse plan [9, 12].

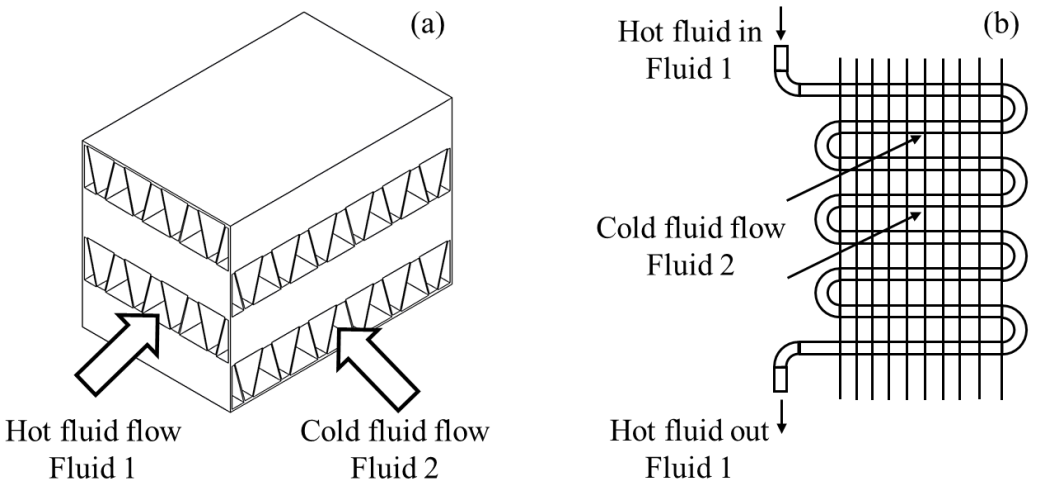

Figure 2.12 Cross-flow arrangement. a) Plate-fin unmixed-unmixed cross-flow exchanger. b) Serpentine tube-fin unmixed-mixed cross-flow exchanger [1, 9]

The common models of cross-flow single-pass arrangement which have been illustrated in Figure 2.13 are as follows:

- Both fluids unmixed
- One fluid unmixed and the other mixed
- Both fluids mixed

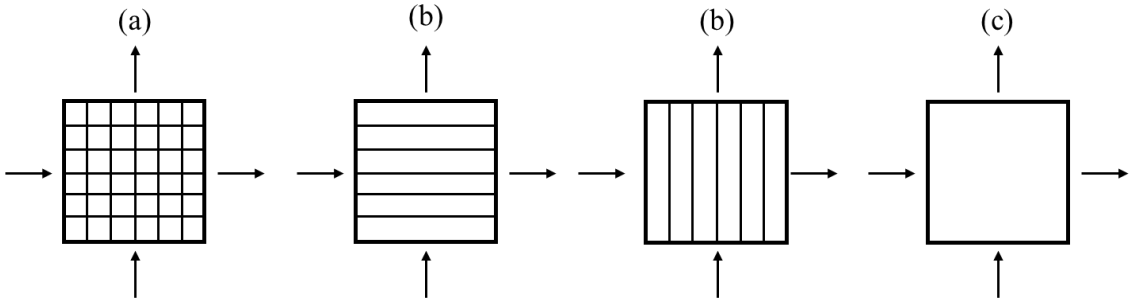

Figure 2.13 Cross-flow arrangement. a) Unmixed-unmixed. b) Unmixed-mixed. c) Mixed-mixed [10]

For an unmixed-unmixed cross-flow arrangement, the two-dimensional temperature distribution is shown in Figure 2.14. As it is illustrated the largest temperature difference exists at the corner where hot and cold fluids enter to the exchanger [9].

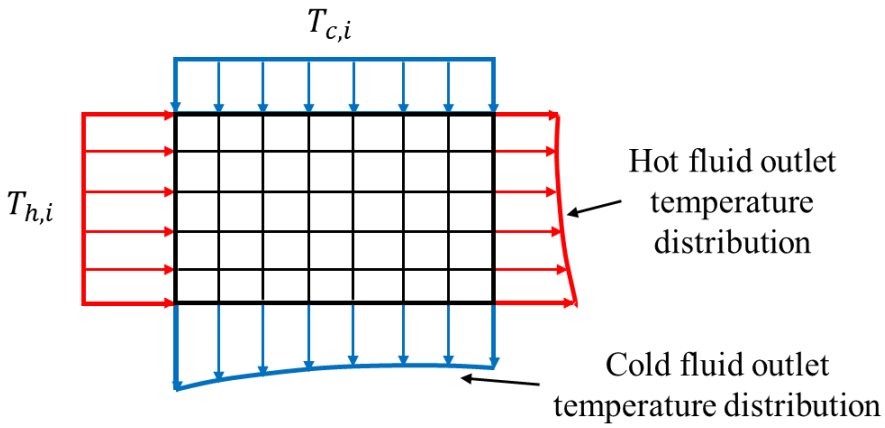

Figure 2.14 Temperature distribution for unmixed-unmixed cross-flow arrangement [9, 10]

2.2 Compact Heat Exchangers

Heat exchangers are also classified according to the compactness. In some applications which are limited by weight and size of exchanger, CHEs are being important. They can be used for variety of applications in automobile and aerospace industries, electronics cooling, waste, and process heat recovery, etc. In this category of heat exchangers, compared to shell-and-tube exchangers, large heat transfer surface area per unit volume is resulting reduced weight, size, support structure and cost. However, CHEs are not necessarily small in size and mass. Furthermore, higher thermal effectiveness is achievable in comparison to shell-and-tube exchangers. Other advantages can be named as easier transportation, better temperature control and less foundation [9, 10].

Generally, CHEs are extended surface exchanger in order to reach higher effectiveness. Gas-to-fluid exchangers in this classification are referred to CHE, where it associated with surface area density (α) greater than 700 m^2/m^3 or a hydraulic diameter (D_h) smaller than 6 mm for operating in the gas flow as shown in Figure 2.15. Therefore, fluids which are employed for CHE application should be relatively nonfouling and clean dur to the small hydraulic diameter. Moreover, according to the small core and importance of pressure drop, the fluid pumping power is as important as heat transfer rate [9, 10].

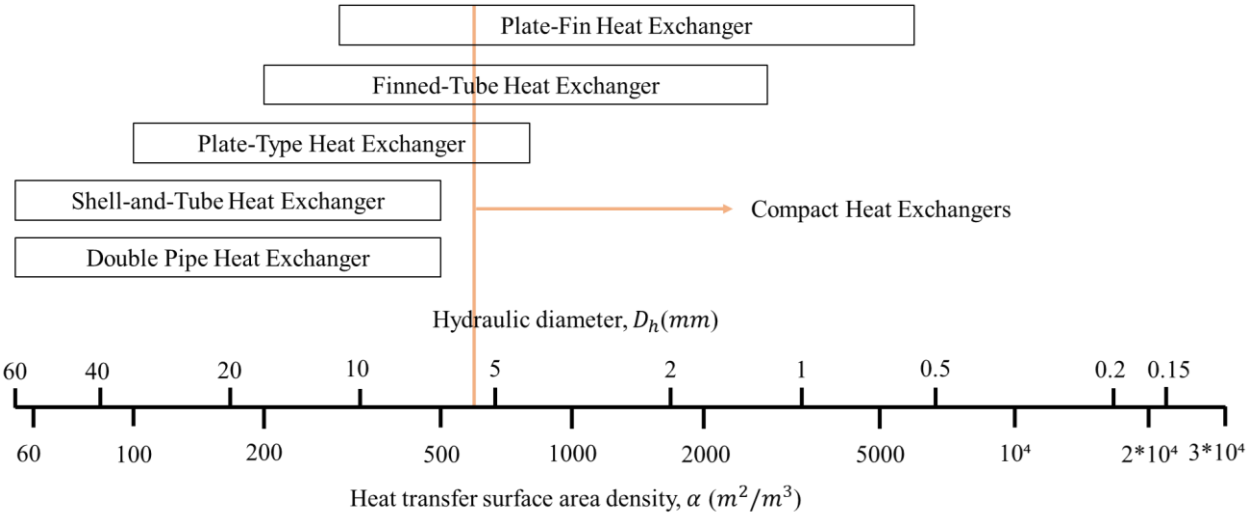

Figure 2.15 Overview of the compactness of exchangers [9]

As CHEs are a classification of the exchangers based on surface compactness, they can be also classified by type of construction. For this matter, basic construction of the CHEs is: Tube-fin and Plate-fin exchangers. Although CHEs can be classified as regenerators, they are employed for gas-to-gas applications which is not documented here. Moreover, basic flow arrangement of the CHEs is single-pass cross-flow [9, 10].

There is various method to construct heat exchangers as compact as possible. The motivation of design for enhanced surface and heat transfer can be used to build a CHE. Generally, enhanced surfaces are used to construct a CHE to reduce overall size and mass. Furthermore, for a given heat transfer rate, reduce pumping power and increase the overall heat transfer rate are the main purpose of the use of enhanced surfaces. Although, enhanced surface can produce the higher heat transfer rate, it can lead to increase core friction and pressure drop. To enhance heat transfer rate in order to build a CHE, large other options exist in different industries based on needs and constrains [19].

2.3 Selection and Requirements of Heat Exchangers

As described in previous sections, number of exchangers are available for different markets and industries and the question is which one is the most appropriate for specific application and given operating condition in terms of construction, compactness, flow arrangement, type of surface, etc. Therefore, there is quantitative and qualitive criteria to select a specific exchanger. Although, it exists number of choices for a particular application, there is one selection which is the best for

given condition. Thus, we should consider number of criteria to choose the best and optimum exchanger [9, 10].

Primary criteria to select an exchanger are the type and phase of fluid that should be handled by exchanger, operating temperature and pressure, heat duty as well as the cost of heat exchanger, for the given operating condition. Considering primary criteria, variety of detail should be granted. These points can be listed as: exchanger material of construction, manufacturing techniques and costs, mass flow rates for hot and cold fluids, flow arrangement, thermal effectiveness and pressure drop and the maintenance after operation [10].

The exchanger must handle the stresses produced by variation of pressure and temperature between two fluids. This produced stress depends to the inlet pressure and temperature of fluids. For example, CHEs are fabricated from thinner material with special manufacturing process, therefore, the operation pressure and temperature are limited in this type of exchangers. Tube-fin exchangers are designed to deal with high pressure inside of tubes if there is only one fluid at high-pressure. Generally, low-pressure fluid on the outside of tubes leads to obtain higher heat transfer rate [9, 10].

Flow rate is another concern to be considered. As the higher flow rate needs the higher cross flow surface area. Furthermore, higher flow area demands the limitation in flow velocity over passages which is limited by pressure drop. Moreover, the number of tubes in the fluid flow direction depends on fluid flow rate as well as pressure drop [9, 10].

Thermal effectiveness and pressure drop are two important factors to select an exchanger for specific application. High thermal effectiveness leads to the high-performance service. On the other hand, unproductive pressure drop should be avoided during design process, as it may impose the pumping cost [10].

Fluid type is also an important factor to select an exchanger under certain operating condition. There will be different combination of fluid phases which deal with exchangers. As an example, in liquid-to-gas exchangers, the heat transfer coefficient on the liquid side is 10 to 100 times of that on gas side, which leads to increase surface area on the gas-side to reach to the thermally balanced design. Therefore, extended-surface exchangers are the common choice for this kind of application [9, 10].

An exchanger should meet normal requirements for design operating condition. These requirements can be listed as: high thermal effectiveness and low pressure drop, Reliability and safe operation, convenient size for easy installation and maintenance, strong construction and light, low coast and simplicity of fabrication and manufacturing [10].

2.4 Heat Exchangers for Aerospace Application

Heat exchangers are employed in many applications to transfer the generated waste heat between fluid flows during a process. In such case, aircraft engines generate heat due to the friction between engine moving components. Therefore, the coolant and oil temperatures in aircraft engines should be controlled carefully to avoid any kind of damage to the engine. To do so, the transferred heat to the oil and coolant liquid must be dissipated through a heat exchanger. Current aero-engines have been reached to the tremendous and cutting-edge technologies in order to reduce fuel consumption and exhaust emission as well as high performance during flight condition. In addition, environmental demands for operating low emission aircraft by airlines, force the engine manufacturer to improve aero-engines in term of Specific Fuel Consumption (SFC). Reaching these goals can be met by incorporating heat exchangers into aero-engines. An exchanger as a recuperator can increase the engine cycle efficiency. As discussed in previous section, design and manufacturing a heat exchanger is a complex duty, since numerous values and factors should be considered such as thermal effectiveness, pressure drop, weight, cost of manufacturing, operating and maintenance, etc., which are more important in aerospace application. In such application, the basic aim is to improve effectiveness and reduce total weight which leads to improve engine efficiency. Therefore, in aero-engine exchangers, the heat exchange should be enhanced versus reduction of dimensions, weight, and hydraulic resistance. As an example, one of the common heat exchanger construction in aero-engines is finned-tube exchangers which can be designed, as compact as possible and, to yield the higher transfer performance and less pressure drop [20-25].

2.5 Methods for the Heat Exchanger Heat Transfer Analysis

If hot and cold fluids outlet temperatures or heat transfer rate are considered as the dependent variables, therefore, these parameters can be related to the independent parameters as represented in Equation 2.1. ϕ represents *function*.

$$\underbrace{T_{h,o}, T_{c,o} \text{ or } q}_{\text{Dependent variables}} = \phi(\underbrace{\underbrace{T_{h,i}, T_{c,i}, C_h, C_c}_{\text{Operating condition variables}}, \underbrace{U, A, \text{Flow Arrangement}}_{\text{Parameters under designer's control}}}_{\text{Independent variables}}) \text{ [9]} \qquad 2.1$$

Where q, U and A represent heat transfer rate in *W*, overall heat transfer coefficient in $W/m^2 \cdot K$ and total heat transfer surface area in m^2, respectively. Six independent parameters as well as three dependent ones for a given flow arrangement can be represented into three dimensionless groups, which are three different method for heat exchangers analysis [9, 15].

- Log Mean Temperature Difference (*LMTD*) method
- Effectiveness-NTU (*ε-NTU*) method
- P-NTU method

The LMTD method is employed when the fluids inlet temperatures are known, and the energy balance expression provides the outlet temperatures. However, if only the inlet temperatures are known, the preferred method to calculate the performance of heat exchanger is the ε-NTU method due to iterative procedure required for LMTD method. In addition, P-NTU method is a variant of ε-NTU method and used commonly for shell-and-tube exchangers, which is not documented here [1, 15]. In ε-NTU method, the effectiveness of the exchanger is a function of heat capacity ratio, C_r, and Number of Transfer Units (*NTU*), which is a dimensionless parameter that is employed for heat exchanger analysis [1].

2.6 Heat Exchanger Optimization

Heat exchangers are designed and used for different applications. Therefore, design and optimization of a heat exchanger involve different criteria. The optimization can be defined using energy rate and cost balance and can be considered as design process. Generally, the optimization is complex task due to the presence of different parameters such as heat transfer performance, pressure drop, outlet temperature as well as size of exchanger. Recent studies demonstrate using of

entropy generation minimization method which allows to combine the effect of pressure drop and heat transfer rate to optimize design parameters for the tube banks. Moreover, recent research establishes applying of the genetic algorithm for optimization of compact heat exchangers to minimize the exchanger volume and cost as well as pressure drop with ε-NTU method [8, 9, 26].

CHAPTER 3 METHODOLOGY OF THE HEAT EXCHANGER CALCULATION

As introduced in section 1.2, the heat exchanger design procedure involves rating and sizing problems. The rating problem refers to determination and evaluation of heat transfer rate, performance and pressure drop for an existing or already sized exchanger. This problem includes exchanger classification according to the compactness, construction and material used, flow arrangement, surface characteristics which involves Colburn-*j* factor and friction factor, fluids mass flow rates, inlet temperatures and fouling factor. However, the sizing problem refers to determination of the physical dimensions of the exchanger. Therefore, for the given heat duty, the sizing problem can be involved parameters such as: fluids flow rates, effectiveness, heat transfer surface area per unit volume, etc., as explained in the literature [10].

Referring to the section 2.5, there will be two main approaches to solve heat exchanger problems, LMTD and ε-NTU methods. Any problem related to the heat exchanger can be employed and represent equivalent results. However, the nature of the problem may lead to the ε-NTU which is easier to implement and more straightforward and useful where at least one outlet temperature is unknown [1, 27].

In this chapter, the reference heat exchanger and assumptions made to perform heat transfer analysis will be presented. Furthermore, the ε-NTU method will be briefly presented and the equations related to the ε-NTU method, total heat transfer rate and CHE relations will be introduced.

3.1 Reference Heat Exchanger: *CF-7.0-5/8J*

In this study, a compact circular staggered tube-circular fin exchanger (see Figure 3.1), surface *CF-7.0-5/8J*, is used as the reference heat exchanger. Where CF refer to the circular fin, 7.0 and 5/8 assign to fin pitch per inch and nominal outside diameter of circular tube, respectively. The letter J refers to the data from Jameson. In case of heat transfer between two fluids in heat exchangers where one of them is gas and the other is liquid, the finned-tube surface configuration is generally used. The exchanger data were provided by Kays, W. M. and London, A. L. following the experimental analysis at Stanford University and at U.S. Navy engineering Experiment Station,

Annapolis, Maryland for steam-to-air tests. The experimental method was performed with a transient test technique. Laboratory experiments method to extract the data of different heat exchangers is presented by Kays, W. M. and London, A. L. in reference [2].

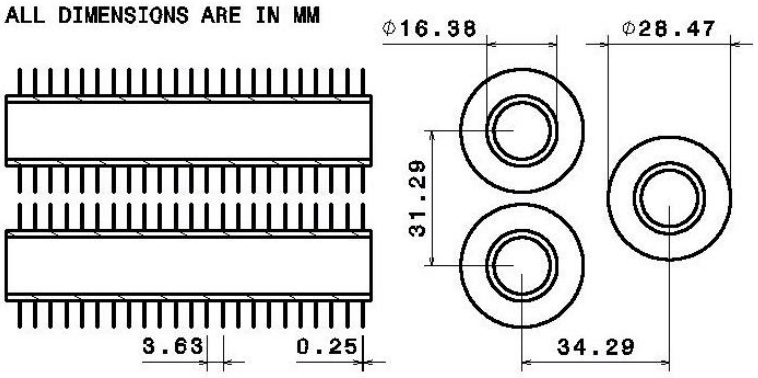

Figure 3.1 Circular staggered tube-circular fin heat exchanger, surface *CF-7.0-5/8J* [2]

Surface geometry of this CHE for laboratory experiments is provided by Kays, W. M. and London, A. L. from the data of Jameson, S. L. in reference [28]. Heat transfer analysis will be performed using the information provided in Table 3.1 [1, 2].

Table 3.1 Surface geometry for *CF-7.0-5/8J*, gas flow normal to the tube banks [2]

Parameters		**Values**
Tube outside diameter	D_o	16.38 *mm*
Fin outside diameter	D_f	28.47 *mm*
Transverse tube spacing	S_T	31.29 *mm*
Longitudinal tube spacing	S_L	34.29 *mm*
Fin pitch	FP	275 per meter
Air-side hydraulic diameter	$D_{h,c}$	6.68 *mm*
Fin thickness	δ	0.25 *mm*
Free-flow area / frontal area	σ	0.449
Air-side heat transfer area / total volume	α	269 m^2/m^3
Fin area / air-side total heat transfer area	A_f/A_c	0.830

Since the surface material is not represented in literature, Aluminum is assumed as the exchanger material. Moreover, Tubes inner diameter is not provided in literature; therefore, it can be considered as a parameter to be investigated.

3.2 Operating Condition

The heat exchanger operating condition is provided by P&WC and should be respected. Due to the classification of U.S. Department of Commerce, this information is subjected to the export control restriction of aerospace and propulsion technology for development and production and can not be disclosed. However, this operating condition is included total heat transfer rate, Hot fluid properties, flow rate and temperatures as well as cold fluid inlet temperature. Therefore, air mass flow rate is considered as a parameter to change and heat transfer analysis on heat exchanger Rating and sizing problems will be performed based on this parameter. For this purpose, an interval of 3 to 8 *kg/s* is expressed for the air mass flow rate. Based on P&WC's suggestion, the proposed interval is a good approximation for all operating condition of this kind of air-liquid cooling system.

3.3 Energy Balance Equation and Heat Transfer

Following by the first law of the thermodynamics, the heat transfer rate from hot to cold fluid can be calculated by applying energy balance to hot or cold fluid as shown in Figure 3.2 [10].

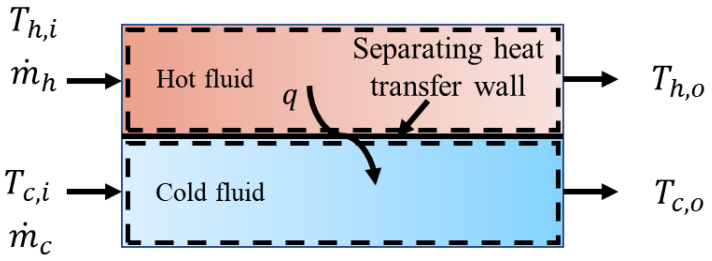

Figure 3.2 Overall energy balance for a two-fluid heat exchanger [1]

The total heat transfer rate, between two fluids is represented by derivation of the steady flow energy equation. Considering negligible potential and kinetic energy as well as negligible radiative heat transfer between the system and surroundings, the Equation 3.1 will give a good approximation of the total rate of heat transfer between hot and cold fluids for any flow arrangement [1, 10].

$$q = \dot{m}_h c_{p,h}\left(T_{h,i} - T_{h,o}\right) = \dot{m}_c c_{p,c}(T_{c,o} - T_{c,i}) \quad 3.1$$

Where q, $\dot{m}$ and c_p are total heat transfer rate in *W*, mass flow rate in *kg/s* and specific heat at constant pressure in *J/kg·K*. in Equation 3.1, fluid heat capacity rate expressed in terms of mass flow rate and specific heat at constant pressure, $\dot{m}c_p$, and represented by the variable C in *W/K*. Therefore, the heat capacity rate for hot and cold fluids will be expressed in Equations 3.2 and 3.3 as following:

$$C_h = \dot{m}_h c_{p,h} \quad 3.2$$

And,

$$C_c = \dot{m}_c c_{p,c} \quad 3.3$$

In a heat exchanger, the heat transfer rate will reach to its maximum value when the hot fluid is cooled to the cold fluid inlet temperature or the cold fluid is heated to the hot fluid inlet temperature as illustrated in Figure 3.3 for a counter-flow exchanger with infinite surface area [10, 12].

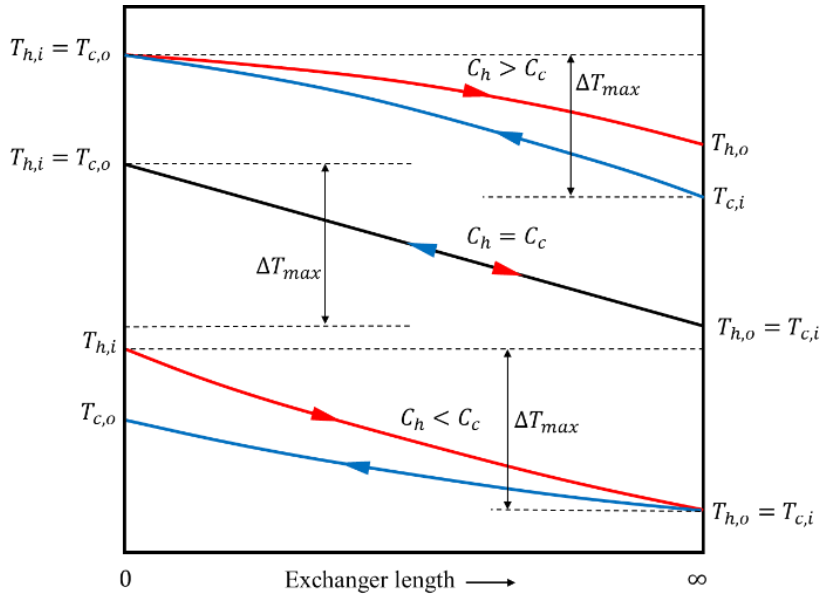

Figure 3.3 Temperature distribution in an exchanger with infinite surface area [9]

This scenario will not happen unless the heat capacity rate of both fluids is identical. As an example, the maximum possible heat transfer rate in a counter-flow exchanger will be reach by a very large

surface with zero longitudinal wall conduction and zero fluid leakage from one to another [10, 12]. The expression for the maximum possible heat transfer rate, q_{max}, will be as follows (Equation 3.4):

$$q_{max} = C_{min}\Delta T_{max} = C_{min}(T_{h,i} - T_{c,i}) \quad 3.4$$

In a two-fluid exchanger, one fluid flow is subjected to the greater temperature change than the other fluid stream. The first stream is called weak stream and the second one is identified as the strong stream, which perform lower (C_{min}) and higher (C_{max}) heat capacity rate, respectively. In other words, in Equation 3.4, hot (C_h) or cold (C_c) fluid heat capacity rate, whichever is smaller, represents C_{min} [1, 10].

3.4 ε-NTU Method for Heat Exchanger Analysis

The ε-NTU was implemented formally by London, A. L. and Seban, R. A. in 1942 at Stanford University, California [29]. In this method, the thermal performance of the heat exchanger is associated with a term called effectiveness ε. The effectiveness changes between 0 to 1, as the actual heat transfer rate in heat exchanger can not be higher than maximum possible heat transfer rate. This term is called also heat transfer effectiveness, effectiveness of the heat exchanger or thermal efficiency. The expression of the effectiveness is defined as the ratio of the actual heat transfer rate in a heat exchanger to the maximum possible heat transfer rate as represented in Equation 3.5. It should be noted that, the effectiveness is the heat transfer rate ratio rather than, the temperature difference ratio [1, 9, 30].

$$\varepsilon = \frac{q}{q_{max}} \quad 3.5$$

In ε-NTU method, there will be two possibilities to find the effectiveness for the specific flow arrangement. The first approach is the mathematical expressions that have been developed for variety of exchangers with a particular flow arrangement. The second approach consists the representation of foregoing expressions graphically [1].

In the first approach, the effectiveness of an exchanger is expressed in terms of heat capacity ratio, C_r, and NTU (Equation 3.6).

$$\varepsilon = \phi(C_r, \text{NTU}, \text{Flow Arrangment}) \tag{3.6}$$

Heat capacity ratio, C_r, is the ratio of lower to higher heat capacity for two fluids involved in heat transfer procedure in a heat exchanger. Therefore, it will be always $C_r \leq 1$. Heat capacity ratio is considered as an operating exchanger variable since C_r depends to the temperatures of the fluids and mass flow rate as represented in Equation 3.7 [9].

$$C_r = \frac{C_{min}}{C_{max}} = \frac{(\dot{m}c_p)_{min}}{(\dot{m}c_p)_{max}} \Rightarrow \begin{cases} \dfrac{T_{c,o} - T_{c,i}}{T_{h,i} - T_{h,o}} & \text{for} \quad C_h = C_{min} \\ \dfrac{T_{h,i} - T_{h,o}}{T_{c,o} - T_{c,i}} & \text{for} \quad C_c = C_{min} \end{cases} \tag{3.7}$$

Number of Transfer Units or NTU is a dimensionless parameter that provides thermal size or heat transfer size of an exchanger. NTU represents the measure of the size of exchanger through overall heat transfer coefficient, U_c, and total air-side heat transfer surface area, A_c as shown in Equation 3.8 [1, 9, 15].

$$NTU = \frac{U_c A_c}{C_{min}} \tag{3.8}$$

The value of the NTU does not demonstrate the physical size of the exchanger necessary. It means, a large value of NTU does not mean the exchanger is large. Although, NTU does not provide the physical size of heat exchanger, it represents a scope of heat transfer area and sometimes can be referred to the exchanger size factor [9, 15].

Correlations to calculate the effectiveness for variety of exchangers were developed and represented in literature [2]. Since in this study, a model will be developed for an air-liquid cooling system for aerospace application and due to the requirements provided by P&WC, a cross-flow exchanger has been chosen. The Equation 3.9 represents heat exchanger effectiveness relation for a cross-flow arrangement. Moreover, in Equation 3.9, NTU can be expressed implicitly as a function of effectiveness and heat capacity ratio and be evaluated by using an appropriate method or iteratively to solve the equation $\phi(NTU) = 0$ [9].

$$\varepsilon = 1 - \exp\left[\left(\frac{1}{C_r}\right)(NTU)^{0,22}\{exp[-C_r(NTU)^{0,78}] - 1\}\right] \qquad 3.9$$

As expressed in the equation above, effectiveness depends to number of transfer units exponentially, at low NTU, the effectiveness is low. By increasing the value of NTU, effectiveness will increase rapidly for small NTU up to 1.5, then, it will be reached to its maximum approximative value but slowly. The larger value of NTU means small increase of effectiveness. Therefore, high performance or high effective heat exchangers are not desirable from economic perspective [1, 2, 10, 12, 27].

The second approach is the graphic representation of effectiveness correlations. Figure 3.4 illustrates the heat transfer effectiveness as a function of NTU and C_r for cross-flow arrangement with both fluids unmixed [2].

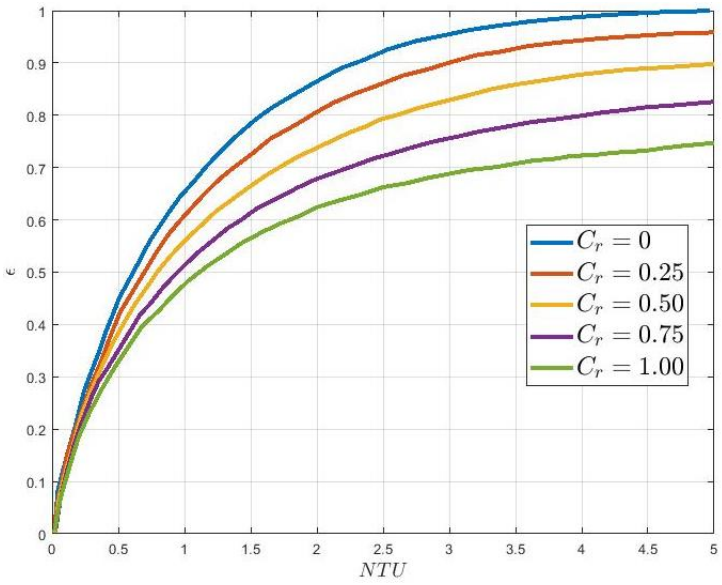

Figure 3.4 Effectiveness of a cross-flow heat exchanger with both fluids unmixed [1]

3.5 Overall Heat Transfer Coefficient

As described in previous sections, a typical heat exchanger is associated with two fluids in different temperatures and it performs heat transfer through a separating solid wall. First, the heat will be transferred from hot fluid to the wall by convective heat transfer. Then, a conduction occurred to transfer the heat through the solid wall. Finally, another convection will pass the heat to the cold

fluid. Therefore, this composite network involves convection and conduction resistances. The overall heat transfer coefficient can be described in terms of either hot or cold surfaces as expressed in Equation 3.10. In the following equation, the term UA refers to the overall thermal conductance in *W/K* [9, 12].

$$UA = U_h A_h = U_c A_c \tag{3.10}$$

Moreover, under operating condition, heat exchanger surfaces are subjected to the fouling by different factor such as: rust formation, fluids impurities or any other chemical reactions between exchanger material and fluids which leads to the corrosion or precipitation of contamination on heat transfer surfaces. These aspects will greatly increase the wall thermal resistance and may introduce additional resistance called fouling factor, R_f in $m^2 \cdot K/W$. In addition, fins can be added to the heat transfer surfaces, especially on the gas-side of the exchanger, to enhance heat transfer rate by decreasing convection thermal resistance. Therefore, fin efficiency may be included in overall thermal conductance. The overall heat transfer coefficient will be represented in Equation 3.11 [1, 12].

$$\frac{1}{UA} = \frac{1}{U_c A_c} = \frac{1}{U_h A_h} = \frac{1}{(\eta_o h A)_c} + \frac{R''_{f,c}}{(\eta_o A)_c} + R_w + \frac{R''_{f,h}}{(\eta_o A)_h} + \frac{1}{(\eta_o h A)_h} \tag{3.11}$$

Where, η_o, h and R_w are fin temperature effectiveness, convection heat transfer coefficient in $W/m^2 \cdot K$ and wall resistance in *K/W*, respectively.

It should be noted that in this study the fouling factor is included to the total heat transfer rate provided by P&WC, therefore, this term is removed from the overall heat transfer coefficient calculation. Considering above-mentioned factors and their impact on thermal conductance, the overall heat transfer coefficient based on cold fluid (air-side) surface area can be reduced and expressed by Equation 3.12 [1].

$$\frac{1}{U_c} = \frac{1}{h_h (A_h / A_c)} + A_c R_w + \frac{1}{\eta_{o,c} h_c} \tag{3.12}$$

Computing the convection coefficient on both side of the separating wall along with calculation of fin temperature effectiveness are required in order to investigate overall heat transfer coefficient.

To do so, the evaluation of Reynolds, Re, and Prandtl, Pr, numbers on both sides as well as Nusselt number, Nu_h, on liquid-side (hot-side) and Colburn-j factor, j_H, on air-side (cold-side) are required.

As represented in previous section, to evaluate the overall heat transfer coefficient for the gas-side, the determination of all thermal resistances is required. In following sections, each thermal resistance term will be calculated with appropriate correlation.

3.5.1 Liquid-Side Convection Thermal Resistance

It can be assumed that the fin thickness is negligible. Therefore, the ratio of the liquid-side surface area to gas-side surface area is shown by the Equation 3.13 [1].

$$\frac{A_h}{A_c} \approx \frac{D_i}{D_o}\left(1 - \frac{A_{f,c}}{A_c}\right) \tag{3.13}$$

Where A_h, A_c, D_i, D_o and $A_{f,c}$ refer to the liquid-side (cold) and gas-side (hot) surface area in m^2, inner and outer diameter of tubes in m and fin surface area in m^2.

To calculate hot-side thermal resistance, the evaluation of convection heat transfer coefficient is required. Therefore, convection coefficient for the fluid inside tubes at constant heat transfer rate can be represented with Equation 3.14 [12].

$$h_h = \frac{Nu_h k_h}{D_i} \tag{3.14}$$

In this equation, h_h, Nu_h, k_h and D_i are convection heat transfer coefficient for fluid flow inside tubes in $W/m^2{\cdot}K$, Nusselt number for the liquid-side, thermal conductivity of the fluid inside tubes in $W/m{\cdot}K$ and tubes inner diameter which is hydraulic diameter for circular tubes in m.

3.5.1.1 Correlation to Determine Nusselt Number

As the internal fluid stream is considered as a steady and incompressible flow in a uniform circular cross-section tubes, thus, fluid mass flow rate is constant and independent from length of tube. Reynolds number on the hot-side (internal flow) can be evaluated by the Equation 3.15 [1].

$$Re_h = \frac{4\dot{m}_h}{\pi D_i \mu_h} \quad 3.15$$

Where Re_h, $\dot{m}_h$ and μ_h refer to Reynolds number for hot fluid inside exchanger tubes, hot fluid mass flow rate in *kg/s* and viscosity of hot fluid in *kg/s·m* [12].

Fluid flow in smooth tubes can be considered as fully developed turbulent flow where Re>10,000. In practice, turbulent flow is used due to its potential for higher heat transfer coefficients. A classical definition for the Nusselt number for fully developed turbulent flow in a smooth circular tube can be obtained from Chilton-Colburn analogy that has been known as the Colburn equation, as represented by Equation 3.16 [12, 31].

$$Nu_h = 0.023 Re_D^{4/5} Pr^{1/3} \quad 3.16$$

However, Dittus and Boelter performed an expression which is slightly different from the Colburn equation. Nusselt number related to the smooth circular tube can be expressed by Dittus-Boeler equation for cooling and heating process. Therefore, the equation associated with cooling which is the case of cooling system is used and represented by Equation 3.17 [1, 32].

$$Nu_h = 0.023 Re_D^{4/5} Pr^{0.3} \quad 3.17$$

Where Re_D and Pr are Reynolds number for a circular tube and Prandtl number, respectively.

3.5.2 Wall Conduction Resistance

In analysis of a heat exchanger, we can perfume the investigation of heat transfer rate under steady state condition and surface temperatures. Therefore, the analogy of the tube wall resistance can be represented with thermal resistance concept. In such case, the heat transfer rate through tube wall is constant in radial direction and can be obtained by Fourier's law. Hence, the conduction in a cylindrical wall which is the tube wall, thermal resistance will be evaluated with Equation 3.18 [1, 12].

$$R_w = \frac{\ln(D_o/D_i)}{2\pi L_w k_w} \quad 3.18$$

Where R_w, L_w and k_w are wall thermal resistance in *K/W*, total tube length in *m* and thermal conductivity of tubes based on its material *W/m·K*. As the length of tubes in heat exchanger is not specified, wall thermal resistance can be evaluated using surface geometry information for existing heat exchanger presented in literature. To do so, the Equation 3.18 will be updated and transformed as represented in Equation 3.19 [1]:

$$A_c R_w = \frac{D_i \ln(D_o/D_i)}{2k_w(A_h/A_c)} \tag{3.19}$$

3.5.3 Air-Side Convection Thermal Resistance

According to the nature of problem which is the analysis of heat transfer process in a CHE for aerospace application, heat transfer for the air-side can be correlated in terms of Colburn-*j* factor, j_H, and Reynolds number, Re. Moreover, temperature effectiveness of the finned surface is required to investigate air-side thermal resistance [1].

3.5.3.1 Colburn-*j* Factor

The design objective, that is included the investigation on heat transfer and flow friction, must be considered for all surfaces. Flow characteristics and heat transfer data for flow normal to banks of finned tubes for several surfaces, such as tubular configuration, are presented by Kays, W. M. and London, A. L. in the format of Figure 3.5 [2].

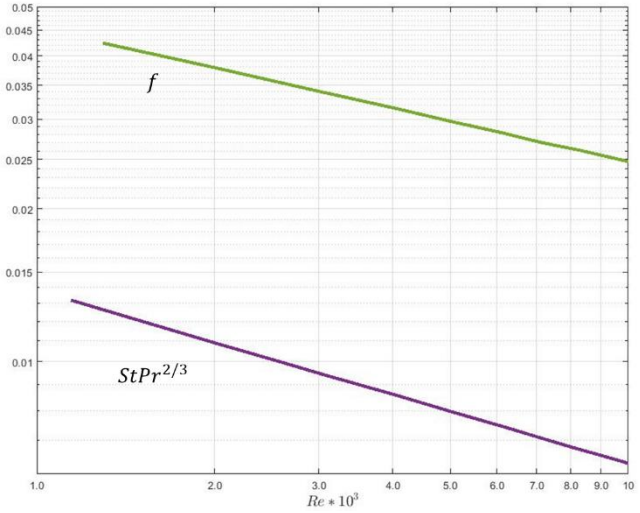

Figure 3.5 Heat transfer and friction factor for circular fin, surface CF-7.0-5/8J [2]

To obtain the value of the Colburn-*j* factor using Figure 3.5, determination of the air-side Reynolds number is required. Therefore, Reynolds number can be calculated by Equation 3.20 which is related to the air-side hydraulic diameter, $D_{h,c}$, in *m*, air viscosity in *kg/s·m* and maximum mass velocity, G_c, in *kg/s·m*^{2} which is determined using Equation 3.21. Therefore, in can be concluded that both Reynolds number and Colburn-*j* factor are based on the maximum mass velocity [1].

$$Re_c = \frac{G_c D_{h,c}}{\mu_c} \tag{3.20}$$

$$G_c = \frac{\dot{m}_c}{\sigma\, A_{fr}} \tag{3.21}$$

Where $\dot{m}_c$, σ and A_{fr} are air mass flow rate in *kg/s*, cross-sectional area perpendicular to air flow direction and exchanger frontal area. Frontal area can be assumed based on pre-design supposition. Then, Equation 3.22 represent Colburn-*j* factor in terms of Stanton number, St, and Prandtl number for the gas-side Pr_c. This equation can be useful commonly for all surfaces where the flow stream is perpendicular to the tube banks. For all gases, Prandtl number can be estimated by air mean temperature and the two-third power is an appropriate approximation for wide range of laminar to the turbulent flow in any kind of cross sectional passage [2, 30].

$$j_H = StPr_c^{2/3} \tag{3.22}$$

Moreover, Stanton number which is a dimensionless heat transfer coefficient can be represented by Equation 3.23.

$$St = h_c / G_c c_{p,c} \tag{3.23}$$

Where h_c and $c_{p,c}$ refer air-side convection heat transfer coefficient in *W/m*^{2}*·K* and air specific heat at constant pressure in *J/kg·K*. By substitution Reynolds number and Colburn-*j* factor into the Stanton number relation, air-side convection heat transfer coefficient, h_c, can be determined as represented by Equation 3.24.

$$h_c = \frac{j_H G_c c_{p,c}}{Pr_c^{2/3}} \quad 3.24$$

3.5.3.2 Fin Temperature Effectiveness

Referring to the Equation 3.12, which leads to determine the overall heat transfer coefficient, the quantity η_o is called temperature effectiveness or overall surface efficiency which describes an array of fins. This term is used for finned surfaces. To determine the effectiveness of the air-side, first the fin efficiency, η_f, must be evaluated. The ideal case is when infinite thermal conductivity or zero thermal resistance exists and entire fin is at the base temperature, thus, fin can dissipate the maximum heat transfer rate. However, in reality, the temperature decrease along the fin, therefore, fin efficiency can be defined by the ratio of the actual heat transfer rate from the fin, q_f, to the ideal heat transfer rate from the fin, $q_{f,max}$, and be represented by Equation 3.25 [1, 12].

$$\eta_f \equiv \frac{q_f}{q_{f,max}} \quad 3.25$$

Furthermore, by considering fin tip convection, fin efficiency can be evaluated by Equation 3.26, approximately [1, 12].

$$\eta_f = \frac{\tanh mL_c}{mL_c} \quad 3.26$$

Where L_c refers to the corrected fin length in *m*, which is equal to $L_f + t_f/2$ for a rectangular fin and m is a factor that is related to the fin shape. Considering the reference heat exchanger, which is a circular fins of rectangular profile exchanger, the factor m will be presented by Equation 3.27. L_f refer to the fin length in *m* and t_f represents fin thickness in *m*. [1, 12].

$$m = \left(2h_c/k_w t_f\right)^{1/2} \quad 3.27$$

Despite the formulation for fin efficiency which are related to the Bessel functions, fin efficiency with tip convection can be defined as a function of $L_c^{3/2}\left(h_c/k_w A_p\right)^{1/2}$ with $A_p = L_c t$ and plotted in Figure 3.6 [1, 12]. A_p refer to the fin profile area in m^2.

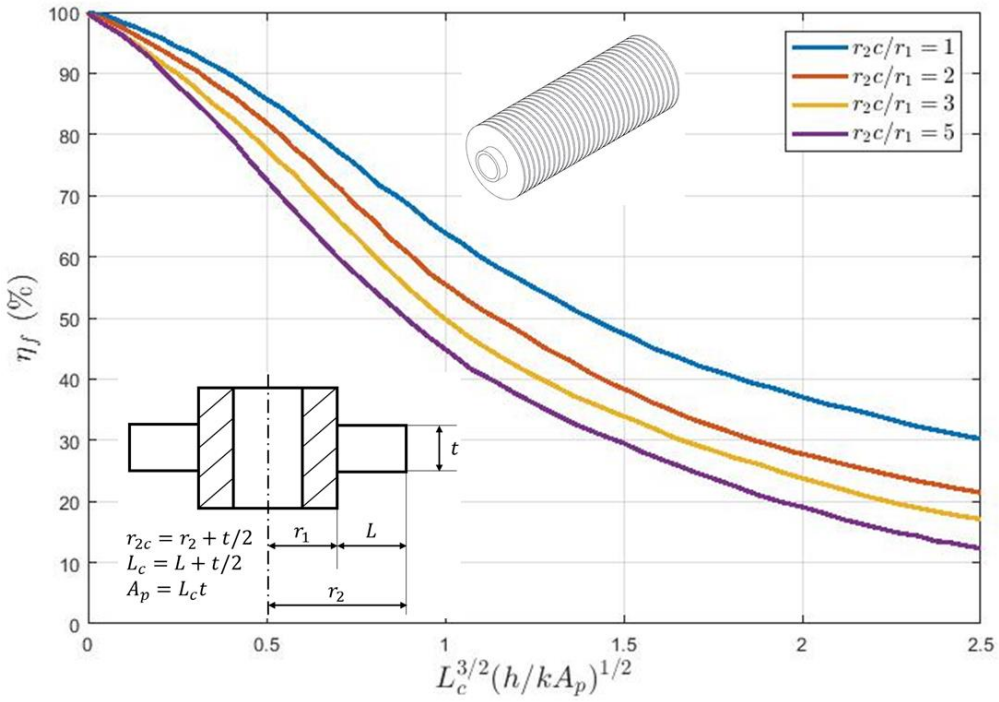

Figure 3.6 Efficiency of the circular fins of rectangular profile [1, 12]

Using fin efficiency, the overall fin temperature effectiveness can be evaluated by Equation 3.28.

$$\eta_o = 1 - \frac{N_f S_f}{A_c}(1 - \eta_f) \tag{3.28}$$

Where N_f, S_f and A are number of fins, single fin heat transfer surface area in m^2 and total heat transfer surface area in m^2, respectively. The ratio of total fin surface area, $N_f S_f$, to total air-side heat transfer surface area, A_c, can be expressed as A_f/A_c and is represented by Kays, W. M. and London, A. L. in literature (see reference [2]). Therefore, fin temperature effectiveness is expressed by Equation 3.29 [1].

$$\eta_o = 1 - \frac{A_f}{A_c}(1 - \eta_f) \tag{3.29}$$

3.6 Heat Exchanger Sizing

During the design process of a heat exchanger, sizing problem refer to the determination of the physical size of exchanger. The task is to study about the sizing parameters for core dimension.

Sizing problem, which is the difficult part of design, involves the evaluation core dimensions to meet the heat transfer rate requirements. Moreover, it can be referred to the sized of already designed/selected exchanger [9]. Therefore, in order to investigate the sizing problem of the heat exchanger, the relations introduced by ε-NTU method in Section 3.4 can be utilized. To evaluate the total air-side heat transfer surface area, A_c, Equation 3.8 may be updated and reduced to Equation 3.30 as follows.

$$A_c = \frac{NTU \cdot C_{min}}{U_c} \tag{3.30}$$

According to the surface geometry provided in literature, total core volume of the heat exchanger can be estimated using α, which is the ratio of the air-side surface area per unit volume of the exchanger [1]. The Equation 3.31 represents the relation to evaluate total exchanger core volume, V_{HX}, in m^3.

$$V_{HX} = \frac{A_c}{\alpha} \tag{3.31}$$

As the frontal area, A_{fr}, was assumed constant, total volume of heat exchanger yields to find the length of exchanger in the direction of air flow using Equation 3.32 [1].

$$L_{HX} = \frac{V_{HX}}{A_{fr}} \tag{3.32}$$

Furthermore, according to the length of the heat exchanger, N_L, the number of tube rows in the direction of air flow will be estimated by Equation 3.33 [1].

$$N_L \approx \frac{L - D_f}{S_L} + 1 \tag{3.33}$$

where D_f is fin diameter in *m* and S_L refer to the longitudinal pitch of a tube bank in *m* as illustrated in Figure 3.7 [1].

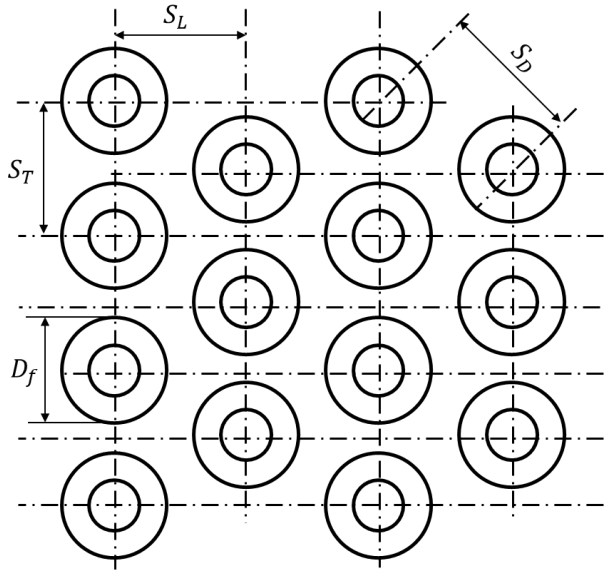

Figure 3.7 Staggered tube bank arrangement [12]

3.7 Pressure Drop Analysis

In many applications, fluid that passes through the core of the heat exchanger needs to be pumped. Therefore, determination of the pumping power is required as a part of Exchanger-Blower system design procedure. The pumping power is a parameter that associated to the exchanger core pressure drop and related to the fluid friction. The heat transfer rate can be affected significantly by pressure drop due to the saturation temperature change if large pressure drop has been occurred. Moreover, pressure drop should be evaluated to avoid and minimize in inlet and outlet and at the same time for an affordable design. Pressure drop is more critical and crucial on the gas side than liquid side. Pumping power is inversely proportional to density ($\propto 1/\rho$). Therefore, for gases the pumping power will have significant influence due to the great impact of density, however, the impact for liquid fluids is minor. The Equation 3.34 represents the expression of pumping power [1, 2, 9].

$$\mathcal{P} = \frac{\dot{m}\Delta p}{\rho \eta_P} \tag{3.34}$$

Where $\mathcal{P}$, $\dot{m}$, Δp, ρ and η_P refer to the pumping power in *W*, fluid mass flow rate in *kg/s*, pressure drop in N/m^2, fluid density in kg/m^3 and pump/blower efficiency.

As mentioned in section 1.1, this thesis deals with the thermal part of cooling system and focus on exchanger characteristics. Therefore, in this section, only pressure drop importance and relations will be introduced.

To evaluate the pressure drop, it can be assumed that air is steady and its properties are independent of time. Moreover, body force caused by gravity is negligible and there are no sources of energy along the fluid flow streamlines. Friction factor is expected as a constant.

The pressure drop consists of two contribution. First, the effects of pressure change that are results of inviscid fluid acceleration or deceleration at inlet and outlet of the exchanger. Second, the pressure losses caused by fluid friction in the core of exchanger. For a selected core geometry, friction factor is a function of Reynolds number as illustrated in Figure 3.5. Accordingly, pressure drop associated with the fluid flow across finned-tube banks can be evaluated by Equation 3.35 [1].

$$\Delta P = \frac{G_c^2 \upsilon_{c,i}}{2}\left[(1+\sigma^2)\left(\frac{\upsilon_{c,o}}{\upsilon_{c,i}}-1\right)+f_c\frac{\alpha V_{HX}\upsilon_{c,m}}{\sigma A_{fr}\upsilon_{c,i}}\right] \qquad 3.35$$

Where G_c is mass velocity in $kg/s{\cdot}m^2$, the quantity σ is the cross-sectional area perpendicular to air flow direction, α is the air-side heat transfer surface area per unit volume, m^2/m^3, A_{fr} represents the heat exchanger frontal area in m^2, V_{HX} is total exchanger core volume in m^3 and f_c refer to the friction factor for a prescribed core configuration. Moreover, $\upsilon_{c,i}$ and $\upsilon_{c,o}$ are specific volumes in m^3/kg for air flow at inlet and outlet and the mean value is $\upsilon_{c,m}$.

3.8 The Implementation of Mathematical Model Using MATLAB

The equations defined in Chapter 3 are implemented in MATLAB environment to investigate heat exchanger design variables as illustrated in Figure 3.8. Using operating conditions provided by P&WC and exchanger surface geometry information that extracted from literature (see reference [2]) the mathematical model calculates parameters related to the rating and sizing problems. These parameters are included the air outlet temperature, heat capacity rate, exchanger efficiency, overall heat transfer coefficient, total air-side surface area, exchanger total volume and pressure drop in terms of air mass flow rate as shown graphically in Figure 3.9.

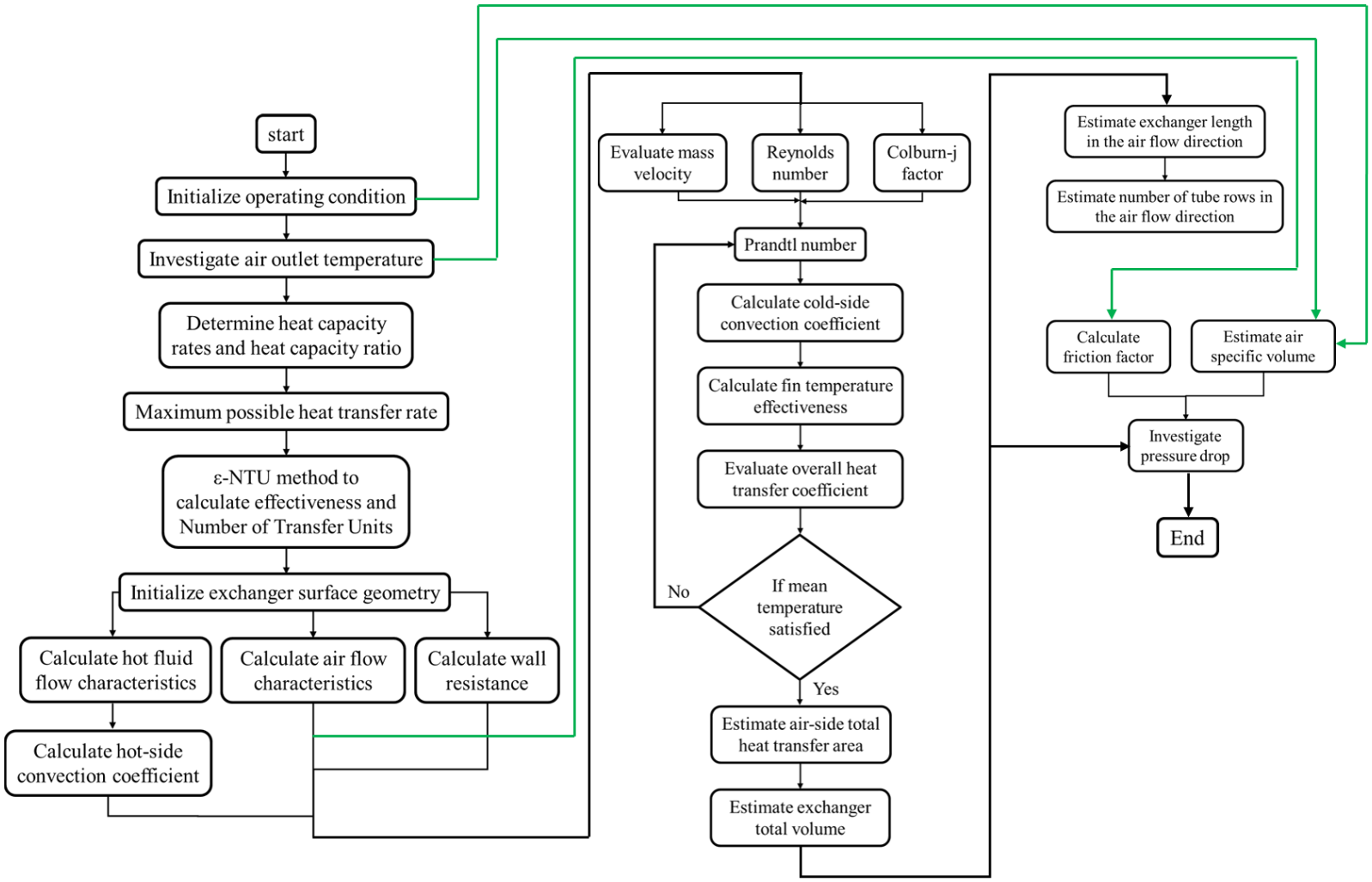

Figure 3.8 Implemented mathematical algorithm using MATLAB

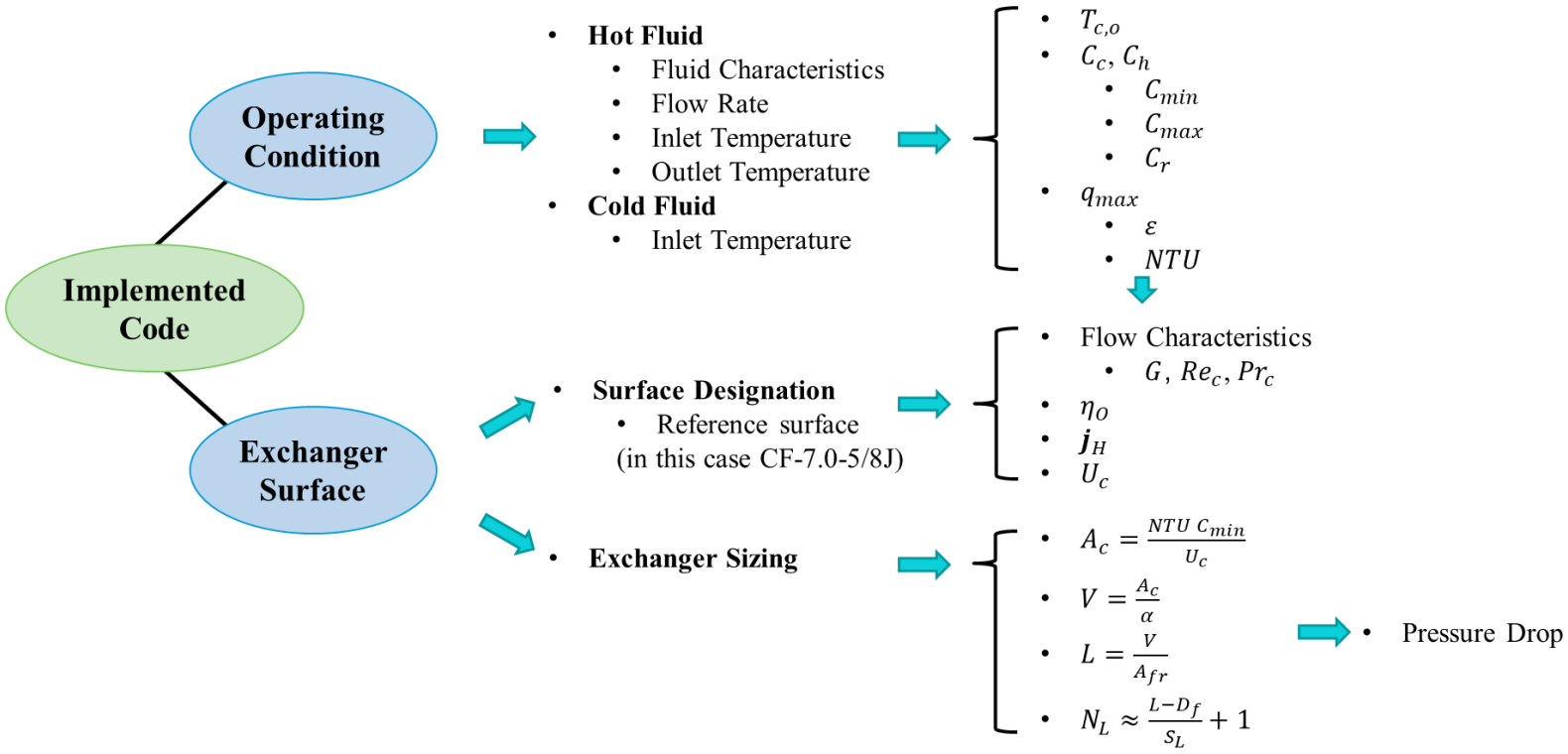

Figure 3.9 Heat exchanger investigated parameters

CHAPTER 4 VERIFICATION

In this chapter, a verification is performed on the mathematical model implemented with MATLAB. The MATLAB code will evaluate the problem analytically and the results can be compared with the solution presented by Incropera et al. in literature.

4.1 Single-Point Verification

The analytical solution represented in literature is for an intercooler that operates in a waste recovery application. Surface geometry is the geometry of reference heat exchanger *CF-7.0-5/8J* as represented in Section 3.1. In this case, the combustion gas and water inside tubes will perform as the hot and cold fluids, respectively. The exchanger will operate under the operating condition as represented in Table 4.1[1].

Table 4.1 Intercooler operating condition [1]

Surface CF-7.0-5/8J			
Combustion Gas (Hot Fluid)		Water (Cold Fluid)	
$\dot{m}_h$	1.25 kg/s	$\dot{m}_c$	1 kg/s
$T_{h,i}$	825 K	$T_{c,i}$	290 K
$c_{p,h}$	1075 J/kg. K	$T_{c,o}$	370 K
μ_h	$338 \cdot 10^{-7}$ Pa. s	$c_{p,c}$	4148 J/kg. K
		h_c	1500 W/m^2

Table 4.2 represents results obtained by MATLAB code and compares with the solution performed in the literature (see reference [1]).

Table 4.2 MATLAB code results vs. solution presented in literature [1]

parameter		**Unit**	**Literature Results**	**MATLAB Results**	**Difference (%)**
Reynolds number	Re_h	-	2740	2744.5	0.16 ↑
Prandtl number	Pr_h	-	0.695	0.695	0.00 -
Colburn-j factor	j_H	-	0.0096	0.0100	4.17 ↑
Friction factor	f_h	-	0.033	0.0358	8.48 ↑
Convection coefficient	h_h	$W/m^2.K$	183	191.15	4.45 ↑
Overall transfer coefficient	U_h	$W/m^2.K$	93.4	95.7	2.52 ↑

Fin efficiency	η_f	-	0.8900	0.8918	0.20 ↑
Fin temperature effectiveness	$\eta_{o,h}$	-	0.9100	0.9102	0.02 ↑
Minimum heat capacity rate	C_{min}	*W/K*	1344.0	1343.8	0.01 ↓
Maximum heat capacity rate	C_{max}	*W/K*	4148	4148	0.00 -
Heat capacity ratio	C_r	-	0.3210	0.3212	0.06 ↑
Heat transfer rate	q	*W*	$3.35 \cdot 10^5$	$3.34 \cdot 10^5$	4.87 ↑
Maximum heat transfer rate	q_{max}	*W*	$7.19 \cdot 10^5$	$7.18 \cdot 10^5$	0.01 ↓
Exchanger effectiveness	ε	-	0.466	0.465	0.09 ↓
Number of Transfer Units	NTU	-	0.65	0.63	1.83 ↓
Combustion gas outlet temperature	$T_{h,o}$	*K*	576.00	575.91	0.02 ↓
Cold side per hot side surface area	A_c/A_h	-	0.143	0.143	0.00 -
Wall conduction resistance	$A_h R_w$	$m^2.K/W$	$3.51 \cdot 10^{-5}$	$3.5131 \cdot 10^{-5}$	0.09 ↑
Mass velocity	G_h	$kg/s.m^2$	13.90	13.92	0.14 ↑
Hot side surface area	A_h	m^2	9.35	8.95	4.23 ↓
Exchanger volume	V_{HX}	m^3	0.0348	0.0333	4.31 ↓
Exchanger length	L_{HX}	*m*	0.174	0.166	4.37 ↓
Number of tube rows	N_L	-	5.24	5.02	4.20 ↓
Pressure drop	ΔP	N/m^2	585.00	612.75	4.74 ↑

As presented above, the MATLAB results were compared with those from solution in literature. Differences between two values where MATLAB solution is higher and lower than the literature result is represented by upward and downward arrows, respectively. The difference between both results is under 5% except for friction factor which is 8.48% Using the Gridded Data Interpolation function to interpolate and extract data from friction factor diagram leads to the mentioned difference which can be considered acceptable.

4.2 Multi-Point Model for Heat Exchanger

Given that the verification for a single-point was performed and the difference between MATLAB code results versus solution presented in literature is under 5%, therefore, the MATLAB solution can be trusted to model the heat exchanger. For the next step, the MATLAB code will be expanded to satisfy the requirements of heat exchanger as well as the operating conditions provided by P&WC.

The multi-point model for the heat exchanger has been coded for a range of cold fluid mass flow. Therefore, the effect of the variation of mass flow on heat transfer rate, effectiveness and the size of exchanger can be investigated.

For the reference heat exchanger, surface *CF-7.0-5/8J*, change of tube inner diameter and its influence on exchanger characteristics will be studied.

CHAPTER 5 RESULTS AND DISCUSSION

In this chapter, the ε-NTU method described in Section 3.4 is applied to simulate and solve rating and sizing problem of reference heat exchanger (*CF-7.0-5/8J*) of the Kays, W. M. and London, A. L as well as study of the pressure drop under the operating condition provided by P&WC. Moreover, the effect of air mass flow and tubes inner diameter variation on rating and sizing matter will be investigated.

First, the proposed method is utilized to estimate the cold fluid flow outlet temperature. Thereafter, the effectiveness and number of transfer units of the exchanger are calculated based on air mass flow. These two steps provide same results for any cross-flow kind of heat exchangers. Second, a code will simulate rating and sizing problem for reference exchanger using data provided by Kays, W. M. and London, A. L. At the end of this chapter, a sensitivity study will be performed on the results of simulation.

5.1 Rating Problem

As mentioned in Section 3.2, equations regarding to heat exchanger rating problem are derived for a range of the cold fluid mass flow of 3 to 8 *kg/s* to satisfy the operating condition provided by P&WC.

5.1.1 Air Flow Outlet Temperature and Effectiveness

According to the hot and cold fluid characteristics, first the cold fluid (air) outlet temperature, $T_{c,o}$, is computed. As represented in Figure 5.1, $T_{c,o}$ is changed from 389.4 to 344.9 *K* that demonstrate air flow outlet temperature will decrease by increasing the air mass flow.

According to the values of the hot and cold mass flow rate and specific heat, hot and cold fluids will represent the maximum and minimum heat capacity rates, which means $C_h = C_{max}$ and $C_c = C_{min}$. However, the code will compute the air-side heat capacity rate for every mass flow rate iteration, air flow heat capacity rate remains as the C_{min}. Moreover, the hot fluid mass flow remains constant, therefore, the hot fluid heat capacity rate has a constant value equal to 29.25 *W/K*. Further, due to the change of the value of air mass flow, $\dot{m}_c$, the value of the minimum heat capacity rate

and heat capacity ratio is changed in every iteration with a constant slope as illustrated in Figure 5.2 and Figure 5.3.

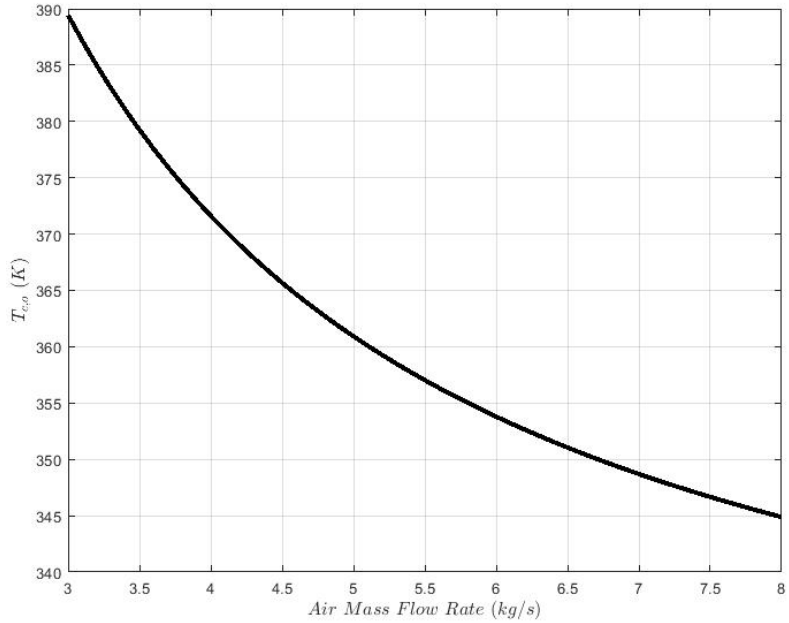

Figure 5.1 Outlet air temperature

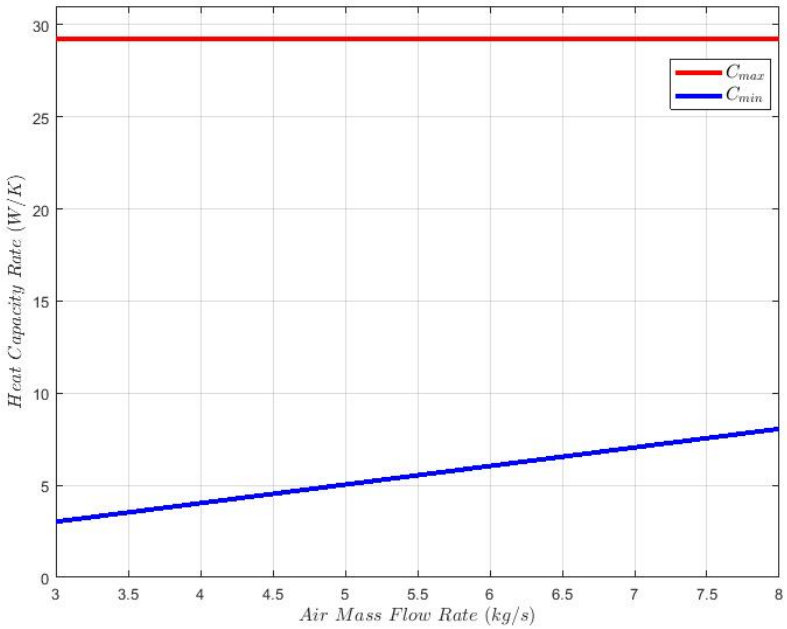

Figure 5.2 Maximum and minimum heat capacity rate

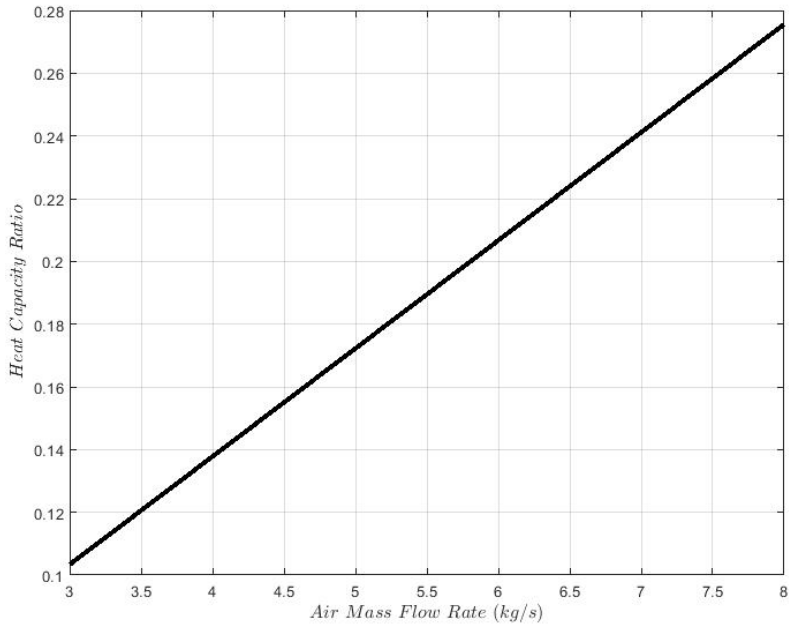

Figure 5.3 Heat capacity ratio

To represent the ε-NTU diagram, a MATLAB function is implemented to find the root of non-linear Equation 3.9; a MATLAB function called *fzero* is used to find the roots of the equation. In MATLAB, *fzero* uses the Brent's method which is a method in root-finding without using derivatives. This algorithm uses a combination of inverse quadratic interpolation, secant and bisection and methods and tries to converge from the neighborhood of zero-crossing [33]. As it exists a C_{min} value associated to q_{max} and C_r in every iteration, therefore, it will be a value of epsilon, ε, and heat capacity ratio, C_r, related to the value of NTU. According to the method chosen, no matter what the type of surface is, the exchanger will experience the same effectiveness due to the hot and cold fluid inlet and outlet temperatures as well as the amount of heat required to extract. As illustrated in Figure 5.4, it can be concluded that for specific C_r, the NTU is reduced with decreasing the value of effectiveness and vice-versa. Additionally, effectiveness decreases by increasing heat capacity ratio for constant NTU. Moreover, by increasing the amount of cooling air stream, the effectiveness of exchanger will decrease (see Figure 5.5).

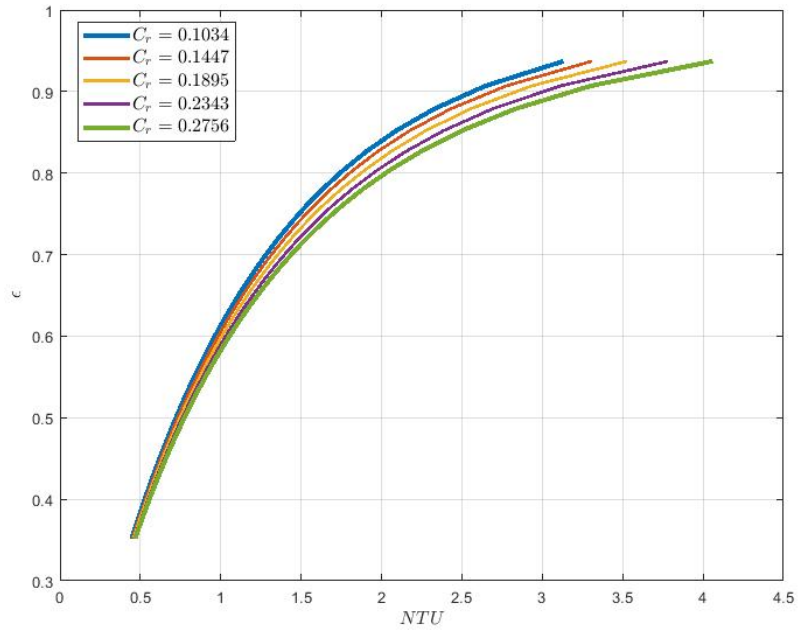

Figure 5.4 Effectiveness of a single-pass cross-flow heat exchanger with both fluids unmixed

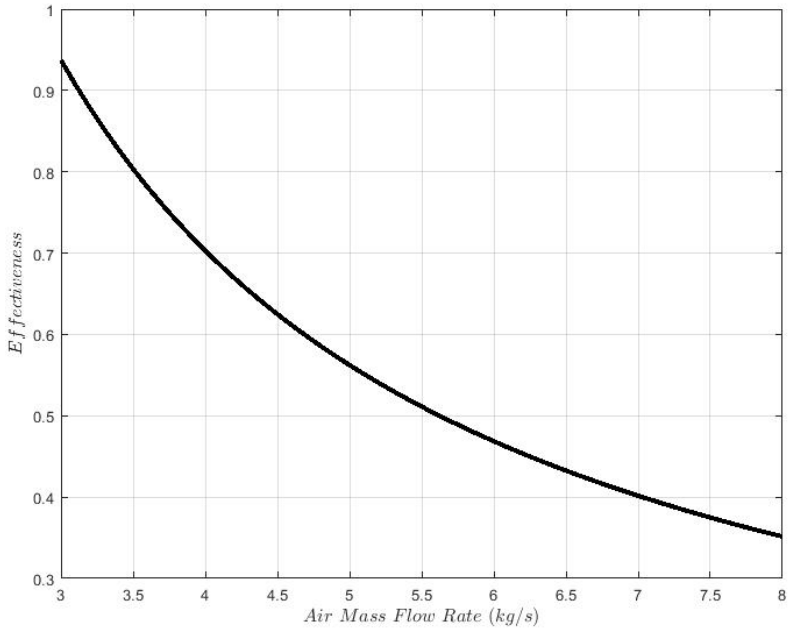

Figure 5.5 Effectiveness of a single-pass cross-flow exchanger in terms of cooling air mass flow rate

5.1.2 Air-Side Overall Heat Transfer Coefficient

As discussed earlier in sections 3.5, the overall heat transfer coefficient is evaluated by Equation 3.12. The overall heat transfer coefficient will be referred to a measure that shows how heat is conducted through a series of convective and conductive layers. Therefore, a larger value shows the easier heat will be transferred through the wall. However, in heat exchanger analysis, the overall heat transfer coefficient depends to the hot and cold side heat transfer surface area as well as convection coefficient. Further, it is a function of wall conduction resistance and fin efficiency [1]. It can be seen in Figure 5.6, by increasing air mass flow rate, the overall heat transfer coefficient increases and reach to its maximum value which is 393.4 $W/m^2.K$ where the air mass flow rate is at its maximum value.

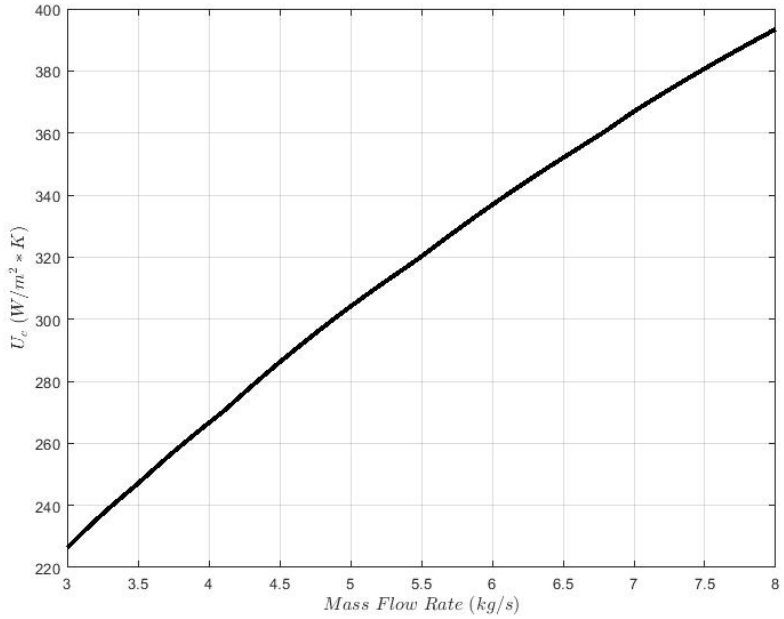

Figure 5.6 Air side overall heat transfer coefficient

According to the Equation 3.12, the first and second terms on right-hand side of equation refer to the liquid-side convection resistance, $1/h_h(A_h/A_c)$, and wall conduction resistance, $A_c R_w$, respectively. Since the hot fluid flow characteristics, provided by P&WC, and surface configuration (*CF-7.0-5/8J*), which represents the wall thermal resistance, do not change during heat transfer process, thus, the two above mentioned terms will not be changed by changing air mass flow rate and remain constant. The last term of this equation refers to the air-side convection

thermal resistance, $1/\eta_{o,c}h_c$. This term depends to the fin temperature effectiveness, $\eta_{o,c}$, and convection heat transfer coefficient, h_c. Convection heat transfer coefficient is a function of air mass velocity, G_c, which represents air mass flow rate, $\dot{m}_c$, and will change by increasing or decreasing air mass flow rate. Although, the air-side convection thermal resistance depends to the fin temperature effectiveness, its effect is minor. Therefore, air mass flow rate plays a significant role on the changes of the air-side overall heat transfer coefficient, U_c and contributes to enforce cooling process.

5.1.3 Influence of Tube Inner Diameter on the U_c

As discussed in Section 5.1.2, convective thermal resistance of hot and cold fluids as well as conductive wall resistance contribute to air-side overall heat transfer coefficient. Given that hot fluid flow characteristics were provided by P&WC, they remain constant and can be changed due to the engine operating condition. Since tube inner diameter is not provided in the literature (see reference [2]), thus, an investigation on tube inner dimeter changes and its effect on air-side overall heat transfer coefficient can be performed.

Referring Equation to the Equation 3.12, tube inner diameter contributes to hot fluid convective and wall conduction thermal resistances. Considering Equations 3.13, 3.14, 3.15 and 3.17, hot-side convective thermal resistance (first term on the right-hand side of Equation 3.12) is proportional to the power of 0.8 of the inner tube inner diameter. It means, increase of tube inner diameter leads to the increase of Nusselt number of hot fluid inside tubes. Since the Nusselt number perform heat transfer along fluid flow layers, larger Nusselt number results more effective convection [12].

Moreover, increase of tube inner diameter will decrease tube wall thickness which leads to the lower wall resistance. In other words, considering Equations 3.13 and 3.19, wall conduction thermal resistance is proportional to the natural logarithm of $1/D_i$, that means the larger the value of the tube inner diameter the less the wall thermal conduction resistance. The effect of tube inner diameter is shown in the Figure 5.7. As seen in this figure, the change of tube inner diameter on overall heat transfer coefficient is almost 7 $W/m^2.K$ and, can be considered negligible.

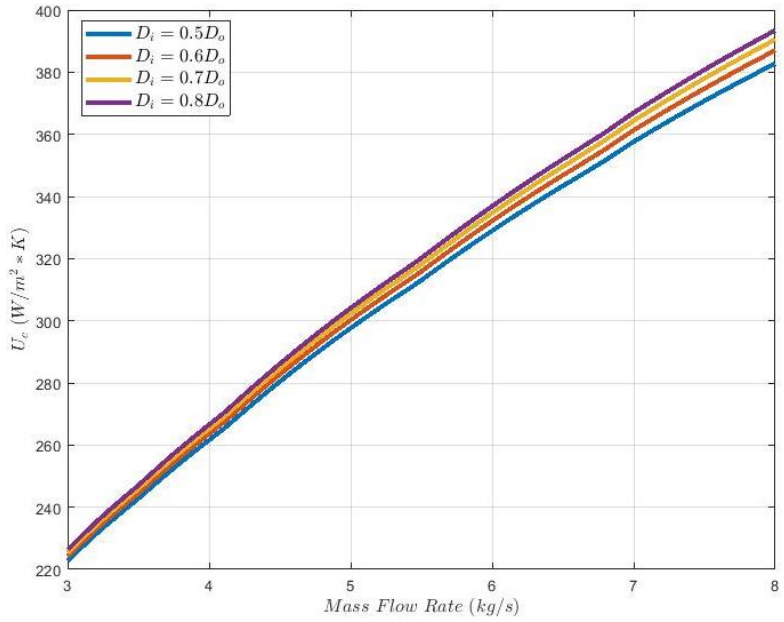

Figure 5.7 Influence of tube inner diameter on air-side overall heat transfer coefficient

5.2 Sizing Problem

As discussed in Section 3.6, sizing problem refer to the determination of the physical size of the exchanger. Since the work has been performed on a selected geometry, the construction and flow arrangement of the exchanger are known. Therefore, the sizing problem will reduce to the estimation of the core dimensions. In this section, the estimation of the total air-side heat transfer surface area and the heat exchanger total volume have been investigated.

5.2.1 Air-Side Total Heat Transfer Surface Area

For the recommended hot fluid outlet temperature and heat transfer rate, air-side total heat transfer surface area, A_c, has been calculated based on the NTU, minimum heat capacity rate, C_{min}, and air-side overall heat transfer coefficient, U_c. Moreover, for the required heat transfer rate and hence the effectiveness, based on knowledge about heat capacity rate on liquid- and air- sides of exchanger, NTU has been determined for the selected flow arrangement. In addition, referring to the core mass velocity and Reynolds number, overall heat transfer coefficient following the convection coefficient is estimated. As seen in Equation 3.30, air-side total heat transfer surface area is inversely proportional to the air-side overall heat transfer coefficient, which means that in

higher air mass flow rate, the overall heat transfer coefficient is getting higher and leads to the better heat transfer rate. Hence, lower air-side heat transfer surface area is required. Decrease of the total air-side heat transfer surface area in terms of air mass flow rate is illustrated in Figure 5.8. it shows that the value of A_c decrease from to 41.83 to 9.564 m^3 with respect to the $\dot{m}_c$.

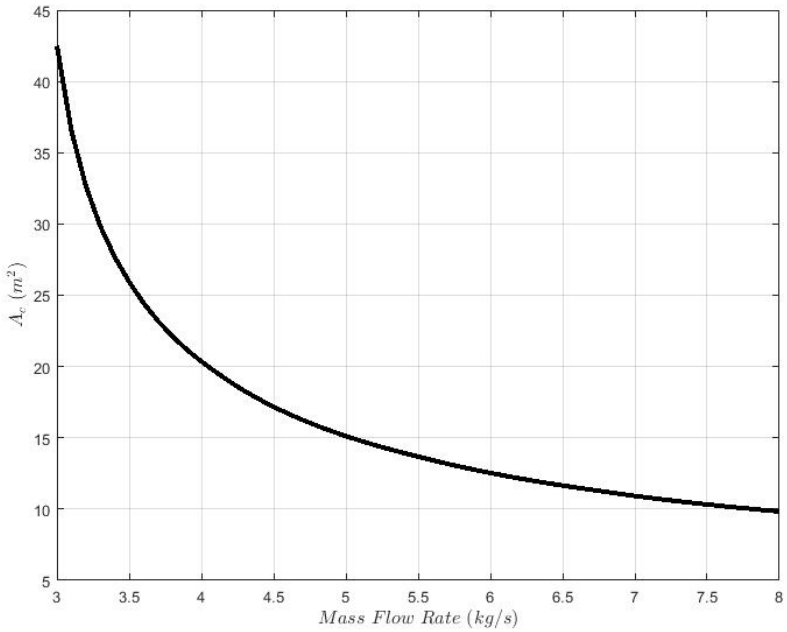

Figure 5.8 Air-side required total heat transfer surface area

5.2.2 Heat Exchanger Total Volume

For the selected surface geometry (*CF-7.0-5/8J*), the ratio of the required air-side heat transfer surface area to total volume which called α, is provided by literature (see reference [2]) and represented in Table 3.1. As mentioned in previous section, air-side heat transfer surface area decreases by increasing air mas flow rate due to the reduction of overall heat transfer coefficient. Total heat exchanger volume is proportional to the air-side heat transfer surface area as shown by Equation 3.31 and will increase or decrease by increasing or decreasing of the heat transfer surface area. Therefore, it will follow the same trend as the air-side total heat transfer surface area. As illustrated in Figure 5.9, heat exchanger total volume decreases from 0.1555 to 0.03557 m^3 with respect to the air mass flow rate.

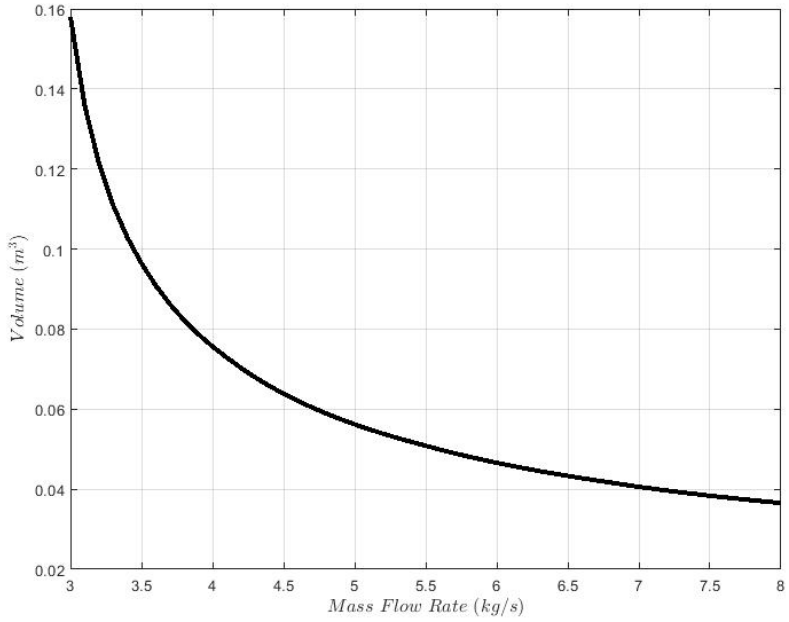

Figure 5.9 Exchanger required volume

5.2.3 Exchanger Length and Number of Tube Rows in the Air-Flow Direction

Referring to the Section 3.6, the frontal area was assumed constant to perform the heat exchanger sizing in the air-flow direction. Considering the heat exchanger total volume, estimation of the length of exchanger in the air-flow direction, L_{HX}, is an easy task to do using Equation 3.32. As illustrated in Figure 5.10, the length of the exchanger will decrease with same pattern as air-side total heat transfer surface area as well as exchanger total volume from 0.7776 to 0.1778 *m*.

Furthermore, according to the length of the heat exchanger, N_L, the number of tube rows in the direction of air flow was calculated by Equation 3.33. Since the number of tube rows depends to the exchanger length, larger exchanger in dimension leads to the larger number of tube rows and vice-versa. As shown in Figure 5.11, number of tube rows in the air-flow direction is represented in the form of step graph since the N_L represents as natural number. Therefore, in MATLAB code implementation, *round* function has been used to round the obtained value to the nearest integer [34]. For the selected exchanger geometry, according to the operating condition. The number of tube row in air-flow direction decrease from 23 to 5 by increasing air mass flow rate from 3 to 8 *kg/s*.

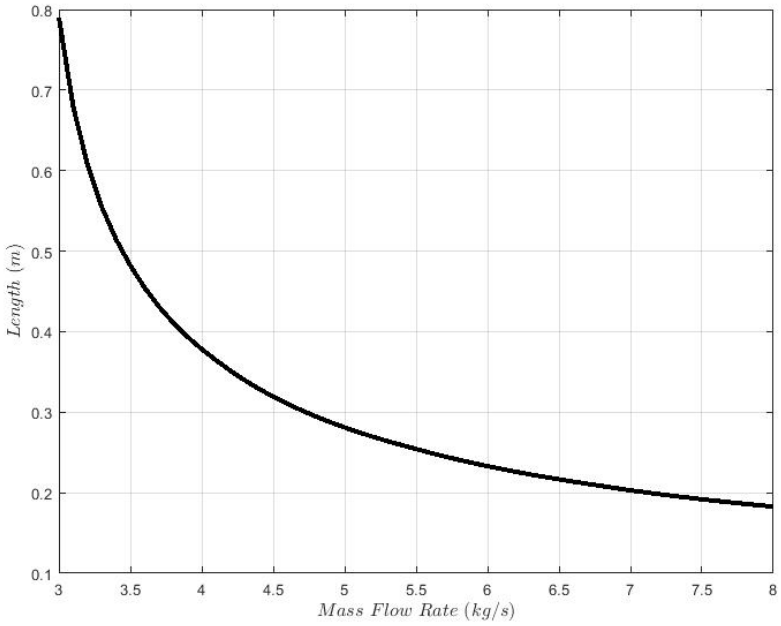

Figure 5.10 Heat exchanger length in the air-flow direction

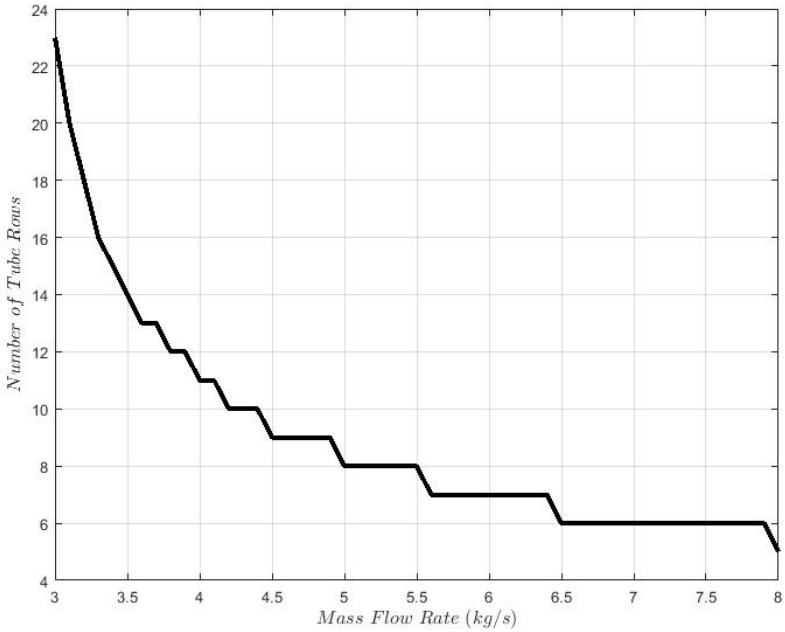

Figure 5.11 Number of tube rows in the air-flow direction

5.3 Pressure Drop

The importance of pressure drop and its influence on pumping power and heat transfer rate were discussed in the Section 3.7. Total core pressure drop depends to the core entrance and exit pressure

losses. At the entrance, pressure loss is associated with frontal area and irreversible free expansion. However, at exit, it will be related to the pressure rise due to the increase of area. Therefore, total core pressure drop includes flowing components: entrance and exit effect, momentum effect and core friction. The core pressure drop due to the friction affect about 90% of ΔP in compact heat exchangers. The relation to estimate the pressure drop associated with the fluid flow across finned-tube banks was introduced by Equation 3.35 and the result obtained by implemented MATLAB code is illustrated in Figure 5.12.

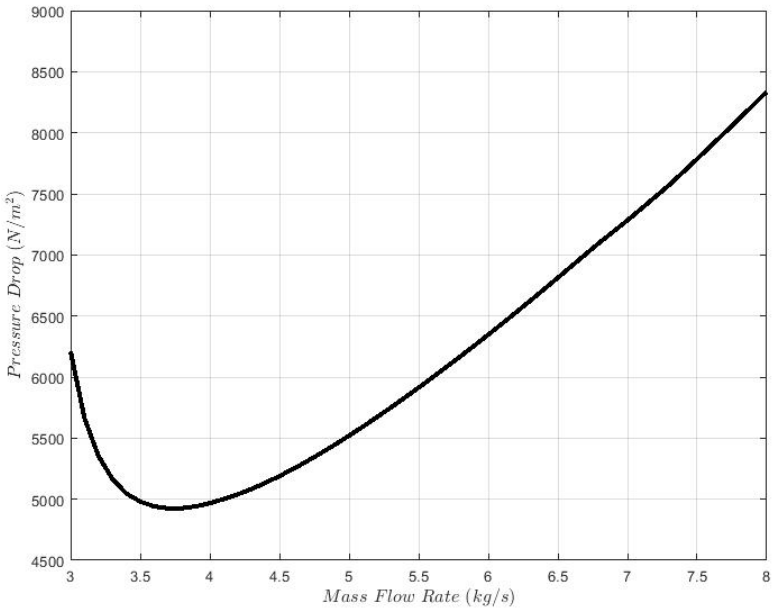

Figure 5.12 Pressure drop associated with gas-flow across circular tube-circular fin tube bank

As shown in Figure 5.12, at low air mass flow rate, $\dot{m}_c$, the effect of core friction due to the core length is higher than that of the mass velocity, G_c. Therefore, at low $\dot{m}_c$, pressure drop decrease by increasing the air mass flow rate up to its minimum value. Pressure drop decreases from $6.208 \cdot 10^3$ to $4.924 \cdot 10^3$ N/m^2 up to the mass flow rate equal to 3.7 kg/s. However, by increasing air mass flow, the mass velocity takes place and its influence on pressure drop will be more significant. Thus, pressure drop starts to rise to its maximum value $8.335 \cdot 10^3$ N/m^2 at 8 kg/s.

Pressure drop is often as important as heat transfer rate; since the higher pressure drop leads to the higher pumping power (and hence more energy required) to maintain desired flow rate. Therefore, the lower the value of pressure drop, the less the pumping power and smaller system [9]. However, in this study, the lowest value of the pressure drop does not demonstrate the best design point. As

illustrated in Figure 5.13, three design parameters have been compared to each other to find an optimum point of the air mass flow rate. Although, the design point for mass flow rate with respect to the exchanger effectiveness and pressure drop is at 5 *kg/s*, where two curves intersect each other, the exchanger itself is large in terms of dimensions. Therefore, the design considering all three parameters can be represent as an interval based on the design criteria and constrains for different applications. It can be noted that this design interval is different for each engine manufacturer and due to the export control classification of aerospace and propulsion technology for development and production, the design interval for P&WC can not be revealed.

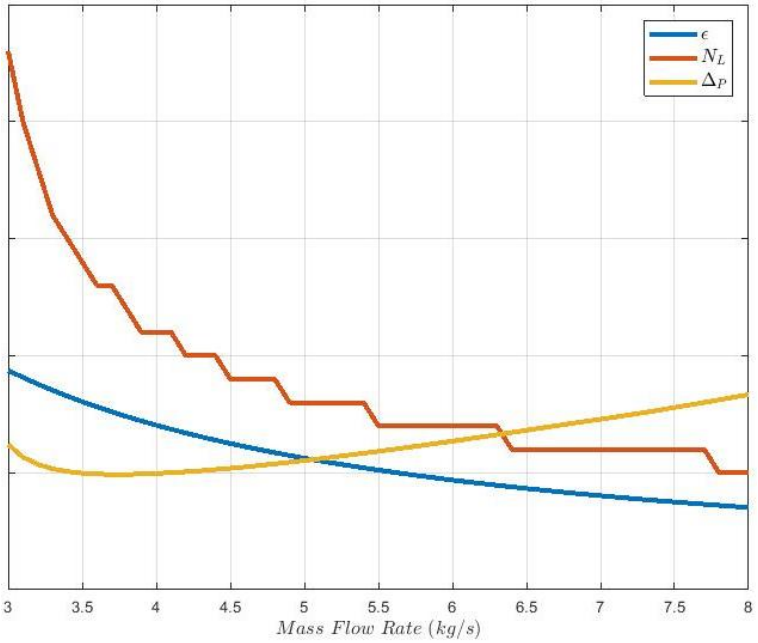

Figure 5.13 Comparison of the exchanger size, effectiveness and pressure drop

5.4 Sensitivity Study

As described in previous sections, the design of a heat exchanger is crucial and depends to the considering numerous parameters and criteria. Therefore, these parameters can play their roles to enhance the heat transfer rate and reach to the optimum design. In this section, the result of a sensitivity study on different parameters will be presented. To do so, four heat exchanger surface geometries have been chosen from literature (see reference [2]) and compared side by side in pairs in terms of specific parameters. First, surfaces *CF-7.34* and *CF-8.72* are compared in terms of the

variation of the fin pitch. Then, surfaces *CF-8.7-5/8J (a)* and *CF-8.7-5/8J (b)* are evaluated in terms of the tube transverse pitch.

5.4.1 Comparison of CF-7.34 and CF-8.72

The comparison of the selected surfaces is about the variation of fin pitch which is the number of circular fins per meter along tubes. Changing the fin pitch does not affect directly on calculation. However, it will affect the air-side hydraulic diameter, $D_{h,c}$, air-side total heat transfer, free flow area per frontal area, σ, air-side heat transfer area per total volume, α, and fin area per air-side total heat transfer area, A_f/A_c. The characteristics of these two surface geometries are extracted from literature (see reference [2]) and represented in Table 5.1. The geometries of both surfaces are illustrated in Figure 5.14.

Table 5.1 Heat exchanger surface geometry, *CF-7.34* and *CF-8.72* [2]

Parameters		**Unit**	**CF-7.34**	**CF-8.72**
Tube outer diameter	D_o	m	0.00965	0.00965
Fin diameter	D_f	m	0.02337	0.02337
Fin thickness	t_f	m	0.00046	0.00046
Longitudinal Pitch	S_L	m	0.02032	0.02032
Transverse Pitch	S_T	m	0.02477	0.02477
Fin pitch (per meter)	-	-	289	343
Air-side hydraulic diameter	$D_{h,c}$	m	0.00476	0.00393
Free flow area / frontal area	σ	-	0.538	0.524
Air-side heat transfer area / total volume	α	m^2/m^3	459	535
Fin area / air-side total heat transfer area	A_f/A_c	-	0.892	0.910

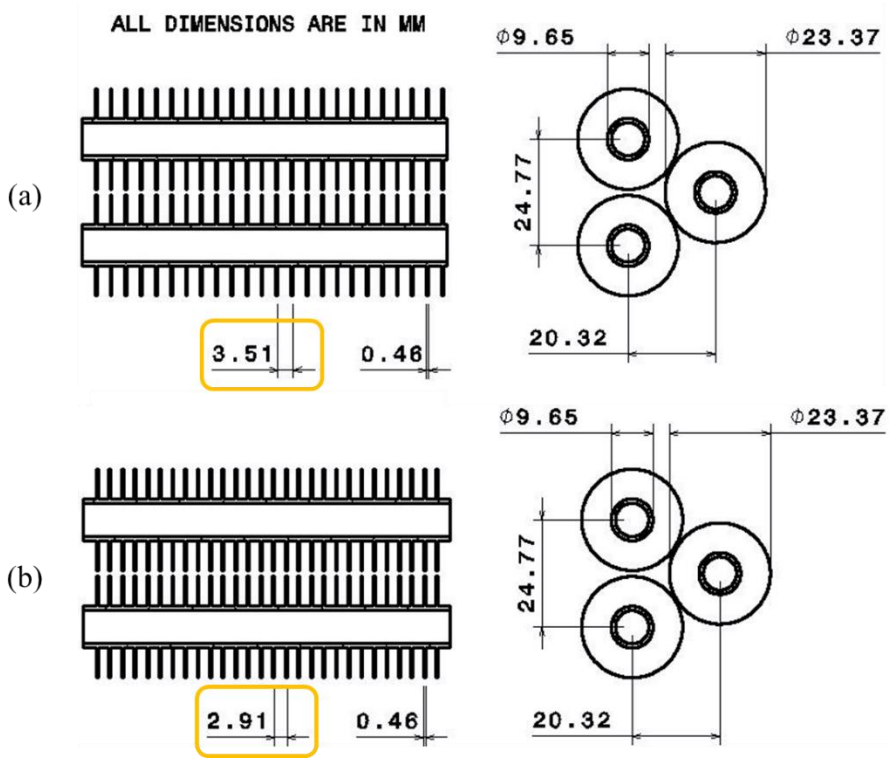

Figure 5.14 Finned circular tubes surface geometries and studied parameter. a) *CF-7.34*. b) *CF-8.72* [2]

The study of the design parameters such as air-side overall heat transfer coefficient, air-side total heat transfer surface area, exchanger total volume and its length as well as number of tube row in air-flow direction and pressure drop have been performed and compared to each other for both surfaces geometry as illustrated in Figure 5.15.

As illustrated in Figure 5.15, increase of fin pitch from *CF-7.34* to *CF-8.72*, leads to the higher heat transfer rate due to the increase of the ratio of cold-side surface area to hot-side surface area (A_c/A_h). Given that the overall heat transfer coefficient in *CF-7.34* is lower than *CF-8.72*, for any mass flow rate, therefore, *CF-7.34* is required higher heat transfer surface area, total volume, length of exchanger as well as number of tube rows in flow direction. Therefore, in can be concluded that higher fin pitch leads to higher heat transfer rate due to the fin density and the exchanger can be constructed in smaller dimensions. On other hand, increase of fin pitch augment the exchanger core friction and leads to the higher pressure drop and higher pumping power which means greater and heavier fan or blower to pump the air.

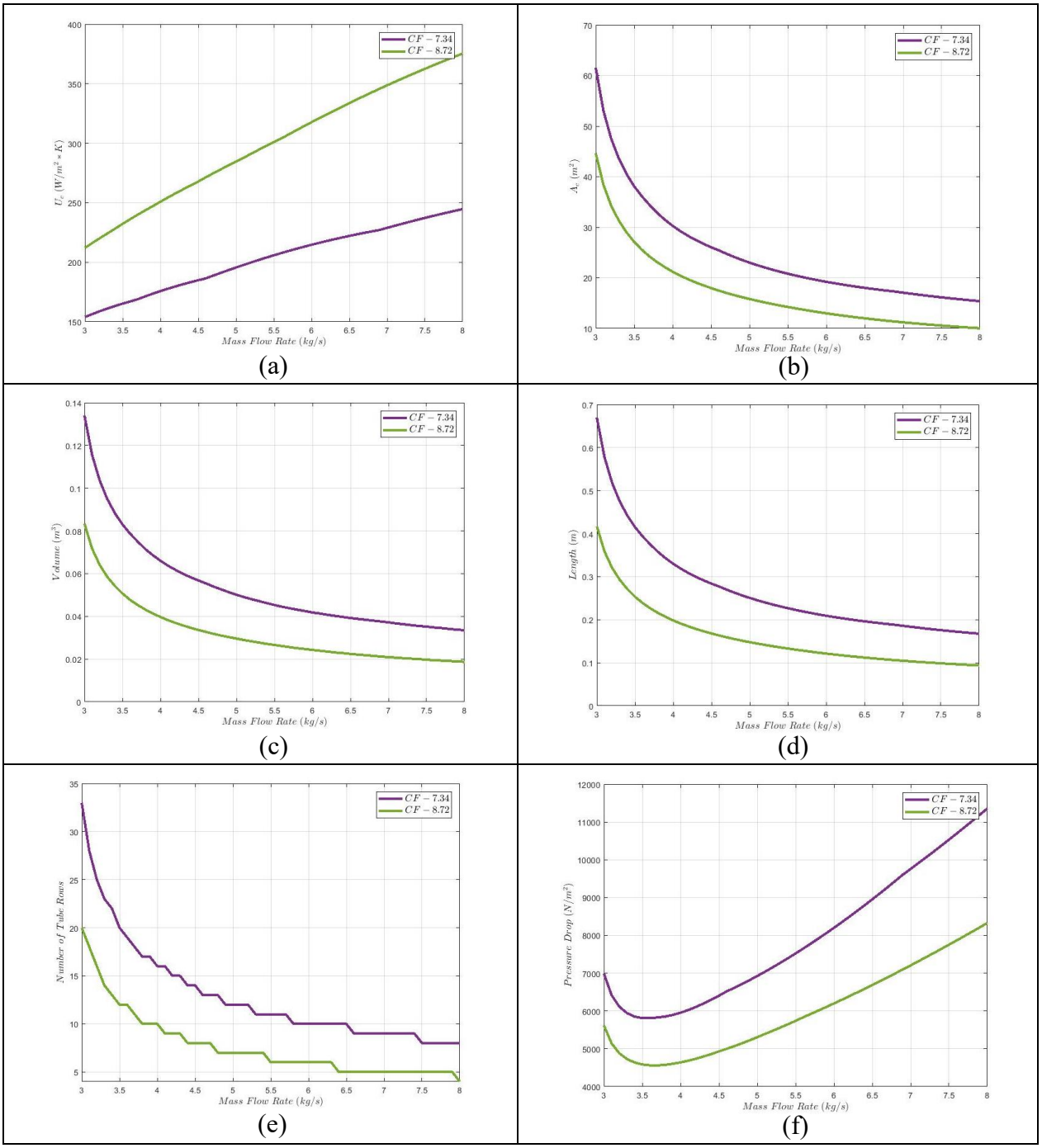

Figure 5.15 *CF-7.34* vs. *CF-8.72*. a) Overall heat transfer coefficient. b) Air-side required heat transfer surface area. c) Required heat exchanger volume. d) Heat exchanger length in the air-flow direction. e) Number of tube rows in the air-flow direction. f) Pressure drop associated with air-flow across circular tube banks

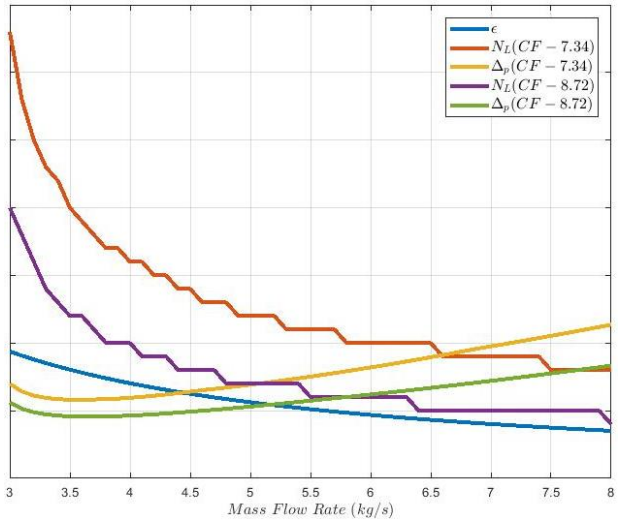

Figure 5.16 Comparison of the exchanger size, effectiveness and pressure drop *CF-7.34* vs. *CF-8.72*

Figure 5.16 illustrates the comparison of size and pressure drop for studied geometries. As seen, at every point of the mass flow rate, surface *CF-7.34* has greater dimension and pressure drop. As discussed, in in Section 5.3, greater pressure drop leads to the greater fan or blower to pump the fluid through exchanger core. Therefore, for a prescribed exchanger effectiveness, surface *CF-8.72* performs better performance regarding to the smaller dimension and lower pressure drop. Since the relative weight for these surfaces is about 1.16, it can be concluded that the larger the fin pitch, the more optimum the exchanger in terms of weight.

5.4.2 Comparison of CF-8.7-5/8J (a) and CF-8.7-5/8J (b)

The other comparison that has been studied is the comparison between two surface geometries of a single family, *CF-8.7-5/8J (a)* and *CF-8.7-5/8J (b)*.

Study was performed on the variation of the tubes transverse pitch, S_T, and its influence on design parameters. Similar to the fin pitch, variation of tubes transverse pitch does not intervene directly into the implemented method. However, its variation changes air-side hydraulic diameter, $D_{h,c}$, air-side total heat transfer, free flow area per frontal area, σ, and air-side heat transfer area per total volume, α. The characteristics of these two surface geometries are extracted from literature (see reference [2]) and presented in Table 5.2. The geometries of both surfaces are illustrated in Figure 5.17.

Table 5.2 Heat exchanger surface geometry, *CF-8.7-5/8J (a)* and *CF-8.7-5/8J (b)* [2]

Parameters		**Unit**	**CF-8.7-5/8J (a)**	**CF-8.7-5/8J (b)**
Tube outer diameter	D_o	m	0.01638	0. 01638
Fin diameter	D_f	m	0.03073	0.03073
Fin thickness	t_f	m	0.00025	0.00025
Longitudinal Pitch	S_L	m	0.03429	0.03429
Fin pitch (per meter)	-	-	343	343
Fin area / air-side total heat transfer area	A_f/A_c	-	0.862	0.862
Transverse Pitch	S_T	m	0.03129	0.04694
Air-side hydraulic diameter	D_h	m	0.005480	0.01167
Free flow area / frontal area	σ	-	0.443	0.628
Air-side heat transfer area / total volume	α	m^2/m^3	324	216

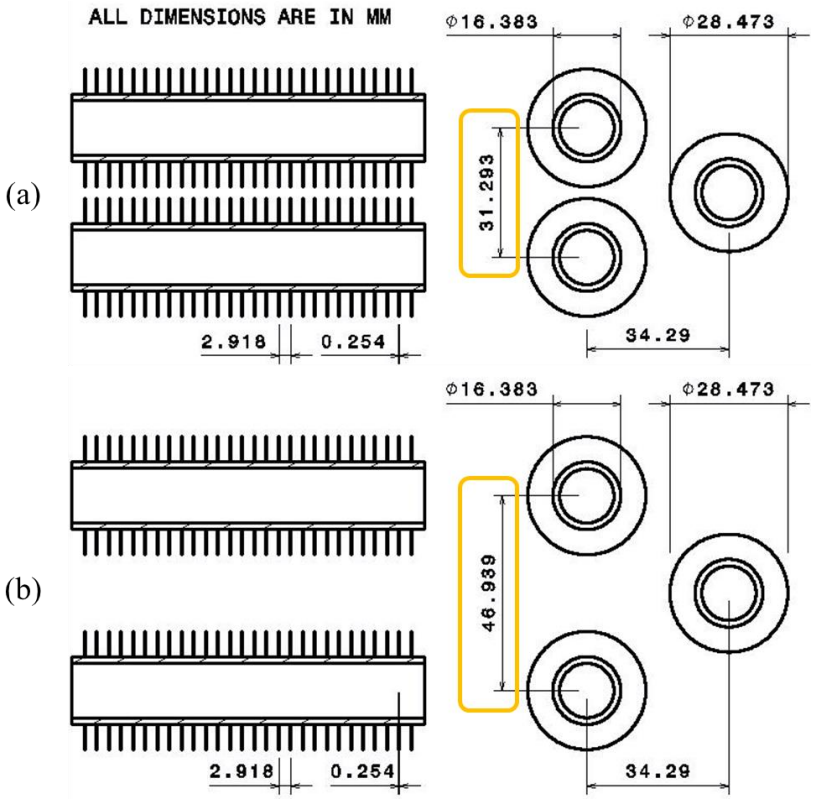

Figure 5.17 Finned circular tubes surface geometries and studied parameter. a) *CF-8.7-5/8J (a)*. b) *CF-8.7-5/8J (b)* [2]

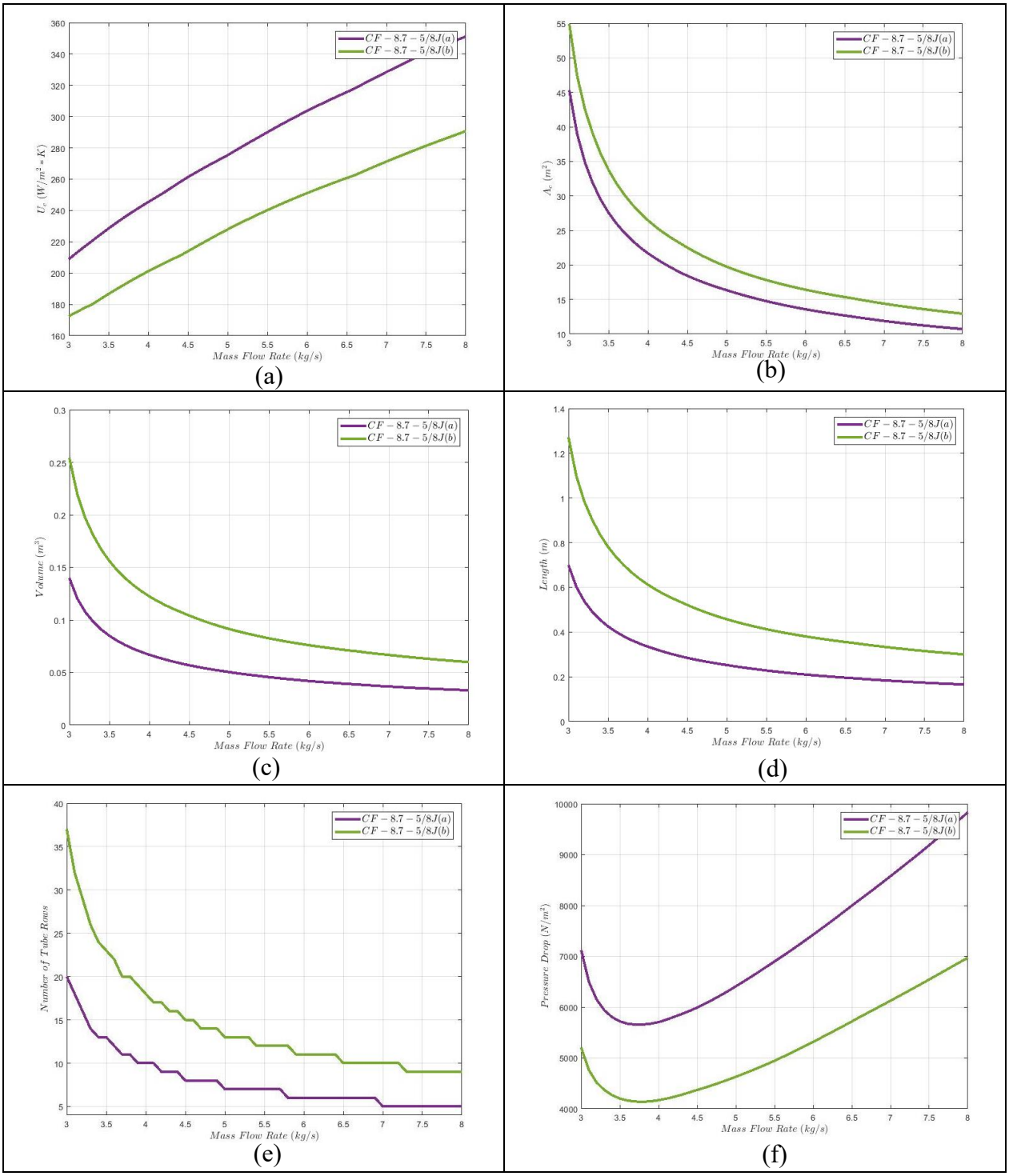

Figure 5.18 *CF-8.7-5/8J (a)* vs. *CF-8.7-5/8J (b)*. a) Overall heat transfer coefficient. b) Air-side required heat transfer surface area. c) Required heat exchanger volume. d) Heat exchanger length in the air-flow direction. e) Number of tube rows in the air-flow direction. f) Pressure drop associated with air-flow across circular tube banks

The study of the design parameters such as air-side overall heat transfer coefficient, air-side total heat transfer surface area, exchanger total volume and its length as well as number of tube row in air-flow direction and pressure drop have been performed and compared to each other for both surfaces' geometry as illustrated in Figure 5.18.

As illustrated in Figure 5.18, increase of transverse pitch from *CF-8.7-5/8J(a)* to *CF-8.7-5/8J(b)*, leads to lower overall heat transfer coefficient following by decrease of air-side convection coefficient due to the increase of the air-side hydraulic diameter. Moreover, by increasing the transverse pitch, hydraulic diameter has more significant influence on Reynolds number than free-flow area per frontal area, σ. Therefore, by increasing transverse pitch, Colburn-*j* factor getting smaller due to the Reynolds number which leads to decrease air-side convection coefficient.

According to the decrease of the air-side overall heat transfer coefficient, for a constant heat transfer rate, heat exchanger physical size must be greater. Furthermore, increase of transverse pitch leads to decrease of the core friction due to the effect of α and σ referring the Equation 3.35 and as a result, pressure drop decrease in higher transverse pitch.

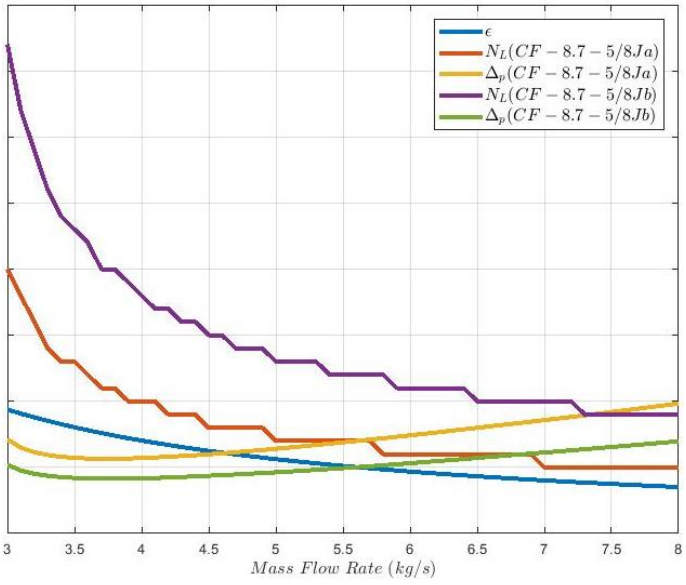

Figure 5.19 Comparison of the exchanger size, effectiveness and pressure drop *CF-8.7-5/8J (a)* vs. *CF-8.7-5/8J (b)*

Figure 5.19 illustrates the comparison of size and pressure drop for studied geometries. As seen, at every point of the mass flow rate, surface *CF-8.7-5/8J (a)* experiences a higher pressure drop than *CF-8.7-5/8J (b)* as its air-side hydraulic diameter is smaller. Therefore, surface *CF-8.7-5/8J (a)* needs to a bigger fan or blower. On the other hand, to reach the same air-side overall heat transfer rate with surface *CF-8.7-5/8J (b)*, bigger heat exchanger is required in terms of physical size due to its lower core relative heat transfer surface density. As the relative weight for these surfaces is about 0.67, it can be concluded that the smaller the transverse pitch, the more optimum the exchanger in terms of weight.

CHAPTER 6 CONCLUSION AND RECOMMANDATIONS

Pratt & Whitney Canada is a major aircraft engine manufacturer that leads the cutting-edge technology development on aerospace production. Improvement of their products in terms of efficiency is crucial to stay in the race of research and development with other manufacturer. As a new long-term plan, P&WC is to introduce a new technology to extend operating rang, reduce fuel consumption and operating cost for different aerospace application. Therefore, as a part of parent project, design and optimization of cooling system is required to overcome the generated engine heat.

In this study the ε-NTU method, which is a straightforward and useful where at least one outlet temperature is unknown, has been implemented to investigate the heat transfer characteristics of a compact heat exchanger. According to the operation condition provided by Pratt & Whitney Canada, an interval for air mass flow rate was chosen to extract different heat transfer characteristics. The method is applied to compute gas-side outlet temperature, overall heat transfer coefficient, exchanger effectiveness and dimensions as well as pressure drop.

A MATLAB code is implemented to solve an intercooler rating and sizing problems as the reference case and output data is verified by the reference case analytical solution. Then, the MATLAB code was expanded to solve a compact heat exchanger.

According to the results obtained from reference exchanger surface which is *CF-7.0-5/8J*, heat capacity rate is increased by increasing air mass flow, however, the effectiveness is decreased due the maximum possible heat transfer rate increase. Furthermore, influence of tube inner diameter on overall heat transfer coefficient was investigated. It demonstrates that the effect is negligible.

Thereafter, the method was used to estimate the air-side heat transfer surface area as well as exchanger volume. It is illustrated that higher air mass flow rate leads to smaller heat exchanger; however, it is not an effective exchanger. Pressure drop was investigated for a range of air mass flow. It is demonstrated that in high mass flow rate which leads to higher pressure drop due to the effect of mass velocity.

Finally, a sensitivity study was performed on four heat exchanger cores to investigate the effect of fin pitch and transverse pitch on heat transfer rate and pressure drop. As illustrated, by increasing the number of fins per meter (fin pitch), overall heat transfer coefficient increases while pressure

decrease. Otherwise, increasing transverse pitch decrease both overall heat transfer coefficient and pressure drop. It is concluded that for a prescribed exchanger effectiveness, large number of the fin pitch performs better performance regarding to the smaller dimension and lower pressure drop. However, the exchanger with smaller transverse pitch experiences higher heat transfer rate and pressure drop due to the heat transfer surface density. To reach the same effectiveness as the exchanger with lower transverse pitch, bigger exchanger is required in terms of the physical dimensions where transverse pitch increases.

Moreover, according to the relative weight of exchangers, higher fin pitch leads to the lower relative weight, while higher transverse pitch leads to the higher relative weight and heavier exchanger. Therefore, it can be concluded that, the optimum exchanger may have higher fin pitch and smaller transverse pitch.

Based on the current study, recommendation for the future works can resumed as follows:

- Apply the correlations concerning Colburn-*j* factor provided in literature to study their accuracy with respect to the experiment data provided by Kays, W. M. and London, A. L in [2] and compared with current study.
- Apply the developed model to investigate the influence of the other surface parameters such as longitudinal pitch and fin thickness.
- Couple the developed model to the air pumping system to investigate global system weight and performance.

REFERENCES

[1] F. P. Incropera, D. P. DeWitt, T. L. Bergman, and A. S. Lavine, *Fundamentals of Heat and Mass Transfer*. Wiley, 2007.

[2] W. M. Kays and A. L. London, *Compact Heat Exchangers*. Krieger Publishing Company, 1984.

[3] P. Epple, F. Durst, and A. Delgado, "A theoretical derivation of the Cordier diagram for turbomachines," *Proceedings of the Institution of Mechanical Engineers, Part C: Journal of Mechanical Engineering Science*, vol. 225, no. 2, pp. 354-368, 2011/02/01 2010.

[4] T. Wright, *Fluid machinery : performance, analysis, and design*. Boca Raton, Flor.: CRC Press (in English), 1999.

[5] V. Dakshina Murty, *Turbomachinery : Concepts, Applications, and Design*, First edition. ed. Boca Raton, FL: CRC Press, 2018.

[6] E. Logan, *Turbomachinery : basic theory and applications*, Second edition, revised and expanded. ed. Boca Raton: CRC Press, Taylor & Francis Group, 2013..

[7] M. Imran, N. A. Pambudi, and M. Farooq, "Thermal and hydraulic optimization of plate heat exchanger using multi objective genetic algorithm," *Case Studies in Thermal Engineering*, vol. 10, pp. 570-578, 2017/09/01/ 2017.

[8] G. N. Xie, B. Sunden, and Q. W. Wang, "Optimization of compact heat exchangers by a genetic algorithm," *Applied Thermal Engineering*, vol. 28, no. 8, pp. 895-906, 2008/06/01/ 2008.

[9] R. K. Shah and D. a. P. Sekulić, *Fundamentals of heat exchanger design*, Hoboken, NJ: John Wiley & Sons, 2003.

[10] T. Kuppan, *Heat exchanger design handbook*, 2nd ed. ed. Boca Raton, Fla.: CRC Press, 2013.

[11] B. Zohuri, "Chapter 12 - Heat Exchangers," in *Physics of Cryogenics*, B. Zohuri Ed.: Elsevier, pp. 299-330, 2018.

[12] Y. Cengel, *Heat And Mass Transfer: Fundamentals And Applications*. McGraw-Hill Higher Education, 2014.

[13] F. Kreith and M. Bohn, *Principles of Heat Transfer*. Brooks/Cole Pub., 2001.

[14] A. Bejan and A. D. Kraus, "11. Heat Exchangers," in *Heat Transfer Handbook*: John Wiley & Sons.

[15] K. S. Ramesh and D. P. Sekulic, "17. Heat Exchangers," in *Handbook of Heat Transfer*, 3rd ed. ed., M. R. Warre, J. P. Hartnett, and Y. I. Cho, Eds. New York: McGraw-Hill Education, 1998.

[16] A. Larowski and M. A. Taylor, "Systematic Procedure for Selection of Heat Exchangers," *Proceedings of the Institution of Mechanical Engineers, Part A: Power and Process Engineering*, vol. 197, no. 1, pp. 51-69, 1983/02/01 1983.

[17] M. A. Taylor, T. Heat, S. Fluid Flow, and G. Plate-Fin Study, *Plate-fin Heat Exchangers: Guide to Their Specification and Use*. HTFS for the Plate-Fin Study Group, 1990.

[18] H. A. Navarro and L. Cabezas-Gómez, "A new approach for thermal performance calculation of cross-flow heat exchangers," *International Journal of Heat and Mass Transfer,* vol. 48, no. 18, pp. 3880-3888, 2005/08/01/ 2005.

[19] C. Ranganayakulu and K. N. Seetharamu, *Compact heat exchangers : analysis, design and optimization using FEM and CFD approach*, Hoboken, NJ: John Wiley & Sons, 2018.

[20] A. A. Mironov, S. A. Isaev, I. A. Popov, R. A. Aksyanov, and A. N. Skrypnik, "Improving the Efficiency of Aircraft Heat Exchangers," *Russian Aeronautics,* vol. 63, no. 1, pp. 147-154, 2020.

[21] D. Saltzman *et al.*, "Design and evaluation of an additively manufactured aircraft heat exchanger," *Applied Thermal Engineering,* vol. 138, pp. 254-263, 2018/06/25/ 2018.

[22] H. Scho¨nenborn, E. Ebert, B. Simon, and P. Storm, "Thermomechanical Design of a Heat Exchanger for a Recuperative Aero Engine," 2004.

[23] J. K. Min, J. H. Jeong, M. Y. Ha, and K. S. Kim, "High temperature heat exchanger studies for applications to gas turbines," *Heat and mass transfer,* vol. 46, no. 2, p. 175, 2009.

[24] C. Albanakis, K. Yakinthos, K. Kritikos, D. Missirlis, A. Goulas, and P. Storm, "The effect of heat transfer on the pressure drop through a heat exchanger for aero engine applications," *Applied Thermal Engineering,* vol. 29, no. 4, pp. 634-644, 2009/03/01/ 2009.

[25] M. Awais and A. A. Bhuiyan, "Heat and mass transfer for compact heat exchanger (CHXs) design: A state-of-the-art review," *International Journal of Heat and Mass Transfer,* vol. 127, pp. 359-380, 2018/12/01/ 2018.

[26] W. A. Khan, J. R. Culham, and M. M. Yovanovich, "Optimal Design of Tube Banks in Crossflow Using Entropy Generation Minimization Method," *Journal of Thermophysics and Heat Transfer,* vol. 21, no. 2, pp. 372-378, 2007.

[27] R. L. Webb and N.-H. Kim, *Principles of enhanced heat transfer*. Boca Raton: Taylor & Francis (in English), 2005.

[28] S. L. Jameson, "Tube spacing in finned-tube banks," *American Society of Mechanical Engineers -- Transactions,* vol. 67, no. 8, pp. 633-642, 1945.

[29] A. L. London and R. A. Seban, "A generalization of the methods of heat exchanger analysis," *International Journal of Heat and Mass Transfer,* vol. 23, no. 1, pp. 5-16, 1980/01/01/ 1980.

[30] W. M. Kays and M. E. Crawford, *Convective heat and mass transfer,* 3rd ed. ed. (McGraw-Hill series in mechanical engineering). New York ;: McGraw-Hill (in English), 1993.

[31] A. P. Colburn, "A method of correlating forced convection heat-transfer data and a comparison with fluid friction," *International Journal of Heat and Mass Transfer,* vol. 7, no. 12, pp. 1359-1384, 1964/12/01/ 1964.

[32] R. H. S. Winterton, "Where did the Dittus and Boelter equation come from?," *International Journal of Heat and Mass Transfer,* vol. 41, no. 4, pp. 809-810, 1998/02/01/ 1998.

[33] https://www.mathworks.com/help/matlab/ref/fzero.html.

[34] https://www.mathworks.com/help/matlab/ref/round.html.

APPENDIX A MATLAB IMPLEMETED CODE

This MATLAB code example was performed for the reference exchanger.

```
%=========================================================================%
%-------------------------Initialize constants-------------------------%

constants;

%=========================================================================%
%-------Calculate air outlet temperature using outlet_temp function-------%

[T_c_o] = outlet_temp(m_dot_c, q, cp_c, T_c_i);

Tm_c_o = mean(T_c_o);
%=========================================================================%
%------Calculate minimum heat capacity & maximum heat transfer rate-------%
%---------------effectiveness and number of transfer units---------------%

[C_min, C_max, C_c, C_h, C_r_vect] =...
    Cmin_Cmax_Cr(m_dot_h, cp_h, m_dot_c, cp_c);

[q_max, epsilon_vect] = qmax_epsilon(C_min, T_h_i, T_c_i, q, m_dot_c);


[NTU, epsilon] = epsilon_ntu(epsilon_vect, C_r_vect);

%=========================================================================%
%------------------------------«CF-7.0-5/8J»-----------------------------%

HX1_main(m_dot_c, A_fr, k_Al, mu_c, T_c_i, cp_c, Tm_c_o, m_dot_h, mu_h,...
    Pr_h, k_h, NTU, C_min);


%=========================================================================%

function HX1_main(m_dot_c, A_fr, k_Al, mu_c, T_c_i, cp_c, Tm_c_o,...
    m_dot_h, mu_h, Pr_h, k_h, NTU, C_min)

    %=====================================================================%
    %---------------characteristics of the heat exchanger----------------%

    D_o     = 0.01638;      % Pipe outside diameter (m)

    D_i     = D_o*0.8;      % Pipe inside diameter (m)

    D_f     = 0.02847;      % Fin Diameter (m)

    t       = 0.000254;     % Fin thickness (m)

    FP      = 275;          % Fin Pitch, #per meter

    D_h     = 0.00668;      % Flow passage hydraulic diameter (m)

    sigma   = 0.449;        % Free-flow area/frontal area

    alpha   = 269;          % Heat transfer area/frontal area (m^2/m^3)

    AfA     = 0.830;        % Fin Area/Total Area (Af/A)

    S_L     = 0.03429;      % Longitudinal Pitch (m)
```

```
%=========================================================================%


% Reynolds number
Re_h = (4 * m_dot_h) / (pi * mu_h * D_i);

% Nusselt number
Nu_D = 0.0265 * (Re_h^0.8) * (Pr_h^0.3);

% Calculate hot-side convetion coefficient,
h_h  = Nu_D * (k_h / D_i);

% Initialize the values of the efficiency of annular fins of
% rectangular profile. Figure 3.19, Page 139.Incropera
[component, r2c_r1, eta] = annular_fin_rectangular_profile;

% Initialize the 3D graphics of the Efficiency of Annular Fins of
% Rectangular Profile (EAFRP) to interpolate
EAFRP = scatteredInterpolant (component, r2c_r1, eta);

% Calculate the parameters of annular fins based on inside diameter
% outside diameter and fin thickness
[r1,~,r2c,~,Lc,Ap] = circular_fin(D_o, D_f, t);

% Ac and Ah are the total gas-side (cold) and water-side (hot) surface
% areas respectively.
% Ah/Ac is the fraction of total gas-side (cold) and water-side (hot)
% surface areas where fin thickness negligible
AhAc = (D_i / D_o) * (1 - AfA);

% Ah*Rw is the wall conduction resistance
AcRw = (D_i * log(D_o/D_i))/ (2 * k_Al * AhAc);

% Initialize the values of the Colburn factor versus Reynolds number
[Reynolds_j, Colburn] = HX1_1_Colburn_Reynolds;

% 2D graphics of the Colburn j factor
Colburn_j = griddedInterpolant(Reynolds_j, Colburn);

% Initialize the values of Prandtl number for air, Table A-4
[T_air_Pr, Prandtl] = Pr_A4;

% 2D graphics of the Prandtl number
Pr_number = griddedInterpolant(T_air_Pr, Prandtl);

col = 1;

for ii = m_dot_c

    % Initialize the factor G based on hot-side flow rate, Sigma and
    % Frontal area where sigma = Free-flow area / frontal area
    G(col,1) = ii / (sigma * A_fr);

    % Calculate Reynolds Number
    Re_c(col,1) = (G(col,1) * D_h) / mu_c;

    % Calculate the Colburn j factor
    jH_KL_c = jH_Colburn_KL(Colburn_j, Re_c(col,1));


    % Iteration mean temperature to find it equal to inlet & outlet
    % temperature average
```

```
    for Tm_c = (2/3)*T_c_i:Tm_c_o


        Pr_air = Pr_number(Tm_c);

        % Calculate cold-side convetion coefficient
        h_c = (jH_KL_c * G(col,1) * cp_c*1000) / Pr_air^(2/3);

        % Calculate efficiency of annular fins of rectangular profile
        eta_f =  eta_annular_rect(Lc, h_c, k_Al, Ap, r2c, r1, EAFRP);

        % Hot-side temerature effectiveness
        eta_o_c = 1 - (AfA * (1 - eta_f));

        % Calculate the overall heat transfer coefficient
        U_c(1,col) =...
            ((1 / (h_h * AhAc)) + AcRw +(1 / (eta_o_c * h_c)))^-1;

        % Try to find Mean temperature equal to average temperature
        if ((T_c_i+Tm_c_o)/2> Tm_c-1 && (T_c_i+Tm_c_o)/2< Tm_c+1)

            break

        end

    end

    col=col+1;

end

    % Gas-side heat transfer surface area (m^2)
    A_c =1000*((NTU .* repmat(C_min', col-1, 1)) ./ repmat(U_c, col-1, 1));

    % Required HX volume (m^3)
    V_HX = A_c / alpha;

    % HX length in the gas-side direction
    L_HX = V_HX / A_fr;

    % Number of tube rows in the flow direction
    N_L = round(((L_HX - D_f) / S_L) + 1);


    %-------------------------------------------------------------------------%
    % Friction Factor, Kays & London

    % Initialize the values of the friction factor vs. Reynolds number
    [Reynolds_f, friction] = HX1_1_friction_Reynolds;


    % 2D graphics of the Colburn j factor
    friction_f = griddedInterpolant(Reynolds_f, friction);


    % Friction factor
    friction_factor_f = friction_factor_KL(friction_f, Re_c);

    %-------------------------------------------------------------------------%

    % Initialize the values of specific volume, Table A-4
    [T_air, sv] = specific_volume_A4;
```

```
        % 2D graphics of the specific volume (SV)
        specific_volume_sv = griddedInterpolant(T_air, sv);


        % Extract inlet, outlet & average specific volume
        [v_i, v_o, v_m] = specific_volume(specific_volume_sv, T_c_i, Tm_c_o);

    %-------------------------------------------------------------------------%

        % Pressure Drop (Pa=N/m^2)

        for jj = 1:length (G)

            for kk = 1:length(V_HX)

            delta_P(kk,jj) = (((G(jj,1))^2*v_i)*0.5)*...
                ((1+sigma^2)*((v_o/v_i)-1)+(friction_factor_f(jj,1)*...
                ((alpha*V_HX(jj,kk))/(sigma*A_fr))*(v_m/v_i)));

            end

        end
end
```